UV/Ozone Surface Treatment of Polymers to Enhance Their Adhesion

Poulis, Johannes A.; Kwakernaak, Adriaan

DOI
10.1002/9781394231034.ch6

Publication date
2024

Document Version
Final published version

Published in
Polymer Surface Modification to Enhance Adhesion

6

UV/Ozone Surface Treatment of Polymers to Enhance Their Adhesion

Johannes A. Poulis* and Adriaan Kwakernaak

Adhesion Institute Delft University of Technology, Faculty of Aerospace Engineering, Delft, The Netherlands

Abstract

The surface treatment of plastics as well as metals or ceramics includes a thorough surface cleaning as an essential step prior to adhesive bonding and coating processes. Besides this, surface activation of polymers is often needed because their surface free energy is too low for durable adhesion of a coating or adhesive. In this chapter various types of UV/Ozone sources with different light spectra as well as the influences of spectra and ozone concentration are investigated and compared. Also the surface wetting and adhesive bond strength as a result of UV/Ozone, atmospheric plasma, or corona treatments on thermoset, thermoplastic, and rubber materials are presented.

UV/Ozone treatment was found to show an excellent cleaning performance on all kinds of materials, and especially as a very useful technique for surface functionalisation of polymers, resulting in durable adhesion both for adhesives as well as coatings. This chapter is a condensed overview of over 30 years of experiments done with UV/Ozone treatments at The Delft University of Technology.

Keywords: UV-light, ozone, atmospheric plasma, corona, contact angle, surface free energy, rubber, CFRP

6.1 Introduction

6.1.1 Adhesive Bonding of Polymers

The generally accepted main criteria for surface treatment for successful adhesive bonding of polymers are: a well cleaned surface, wetting capability

**Corresponding author*: j.a.poulis@tudelft.nl

K.L. Mittal and A.N. Netravali (eds.) Polymer Surface Modification to Enhance Adhesion: Techniques and Applications, (199–272)

(high surface free energy), homogeneity, roughness, and stability (no weak boundary layers). Moreover, spreading of the adhesive is the minimum requirement to allow molecular interactions and physical adsorption. For this reason, polymers in general (and polyolefin in particular) are difficult to bond because of the absence of polar or reactive groups on their surfaces and their low surface free energy. Surface treatment (without affecting the bulk properties of the polymers) to increase the surface free energy is thus an essential and critical part of the adhesive bonding, sealing or coating processes and to impart reactive chemical groups on polymer surfaces (surface modification, functionalisation) to enhance their adhesion characteristic [1, 2].

Throughout the last century a large number of polymer surface modification methods have been developed and commercialised (Table 6.1) all with their specific pros and cons. They can be divided into three main groups: physicochemical (e.g. laser, flame, plasma, corona, and UV/Ozone treatments), chemical only (e.g. pickling, etching, ozone gas exposure), or mechanical (e.g. grit blasting, grinding) surface treatments. Physical and chemical methods are mainly applied to increase the surface free energy and microroughness, while mechanical treatments can only create a fresh clean and chemically active surface, by removing the upper surface layers, creating an increased surface area to allow more interactions on a molecular scale and optimize the topography to make mechanical interlocking possible [2, 3].

6.1.2 UV-C Sensitivity of Polymers

Surfaces of organic materials, and especially those of non-pure (commercial) polymer and rubber blends, are in contrast to metals, far more dynamic with the additional probability of a greater surface variation which might affect the adhesive bond strength. The atomic bonds of organic materials (such as rubbers and polymer blends) are sensitive to UV-C light, especially in combination with reactive gas species like ozone, causing visually a loss of shine or gloss (etching) and often colour change (yellowing) as a result of cross-linking, chain scissions and oxidation [3]. The formation of functional groups during such processes will lead to an improvement in adhesion property. However, the sensitivity to UV-C light can be (strongly) reduced when small weight percentages of UV- scavengers and/or filler materials such as carbon black are added, which absorb the photon energy [4, 5]. Even these polymer blends were often found to be susceptible to UV-C light in combination with ozone gas and could be successfully treated for improved adhesive bonding.

Table 6.1 UV/Ozone surface treatment of polymers compared to other surface treatment techniques. +++: excellent, ++: very good, +: good, +/- average, -: disappointing, --: bad, ---: very bad, n.a.: not applicable.

	Surface treatment						
	Physicochemical				**Chemical**	**Mechanical**	
	UV/Ozone	**Atm. Plasma**	**Vacuum plasma**	**Corona**		**Blasting**	**Grinding**
Removing small traces of surface contamination	+++	-	+++	-	+++	---	---
Surface activation	+++	++	+++	+	++	n.a.	n.a.
Complex substrate shape	---	++	+++	++	++	++	++
Activation speed	-	+++	--	+	+	n.a.	n.a.
Low investment costs	+++	+/-	---	+/-	--	+/-	+++
Low running costs	+++	++	+/-	++	--	+	+
Reproducibility	+++	++	+++	++	+++	++	++
Environmentally friendly	+++	+++	++	+++	--	-	-

Adhesive bonds of industrially blended polymer products that will definitely fail at the interface, even after an initial successful UV/Ozone surface treatment, are those which include a (low molecular weight) release agent which diffuses from the polymer bulk to the surface as a function of time, leading to adhesive bond failure. Another group of materials which are impossible to pre-treat by UV/Ozone for improved adhesive bonding are the fluorpolymers, Teflon® being the best known, and will definitely show adhesion failure.

Environmental regulations and the development of new materials as substrates and the aim for improved (environmental) performance are a constant driving force to improve or fine-tune existing chemical and physical surface treatment processes for an optimum adhesive bonding. To minimize liquid waste during such processes, dry surface modification techniques combining oxygen plasma and an ultraviolet light source are often employed. They form oxygenated functional groups on the polymer surface, making it more hydrophilic and thus more amenable to adhesion. One of these methods employed at low pressure is known as vacuum UV (VUV) with wavelengths ranging from 100 to 200 nm [3].

This chapter, however, mainly focuses on dry physicochemical surface treatment processes during which UV-light is generated by a low cost low pressure mercury or an Excimer lamp in a laboratory environment as an alternative to the more sophisticated and more well-known chemical surface treatments as mentioned above. They were applied in combination with ozone gas to improve wetting of polymer surfaces by increasing the surface free energy.

6.1.3 UV/Ozone Treatment: Advantages

One of the major advantages of the UV/Ozone cleaning/surface activation process is that after a simple cleaning by either soap and water or a solvent (and removal of the inactive oxide layers in the case of metal treatment) no further chemicals are needed before a successful adhesive bonding, printing, or coating can take place. This makes the UV/Ozone process an environmentally-friendly alternative treatment method for adhesive bonding of inert polymer materials such as Ethylene-Vinyl Acetates (EVAs) as used in the shoe industry, and will further help to abandon the use of hazardous chemicals [6, 7].

Though not widely reported in literature, the use of UV/Ozone equipment for surface cleaning of non-polymeric surfaces is found to give excellent results [8], even better when compared to other far more popular methods (Table 6.1). This technique has been described as very effective for durable adhesive bonding of plastics and rubbers, as well as for metals, specifically in combination with sol-gel and water-based primers [9–13].

A major advantage of the UV/Ozone treatment, as described below, is the fact that it is very reproducible, as a result of the limited number of variables involved, the most important ones being the distance between surface and UV-source; the source power, spectrum and its age; and the concentration of ozone gas used. The equipment itself is easy to use (simply on/off) and is low cost [14]. Finally, the process can take place at room temperature and is environmentally-friendly, leaving no hazardous (solid or liquid) waste, as the small amount of organic surface contamination leaves the process as volatile molecules such as CO_2, H_2O, NO_2, and N_2.

6.1.4 UV/Ozone Treatment: Disadvantages

The biggest disadvantage of the UV/Ozone cleaning/ surface functionalisation technique is that non-flat or 3D-shaped substrates are difficult to treat. However, McIntyre and Walzak explored the possibility to make use of separate UV-light and ozone generators to treat 3D shaped objects [15].

Another disadvantage of the technique is that the treatment is rather time consuming, though the efficiency (treatment speed) can be improved when the concentration of ozone gas and/ or the UV intensity/cm^2 is increased [16, 17]. For example, by adding polished aluminium reflectors (Alzak) to focus the light on the surface of the object.

Another minor disadvantage might be that often a cleaning step of the surface by either a solvent or soap solution should be done prior to the UV/Ozone treatment to improve reproducibility. Otherwise, one is simply oxidizing surface contaminants which will result in an improved surface wetting, but might very well lead to unexpected bond failures.

The next sections are an assembly of experimental data based on 30 years research on surface cleaning and activation mainly done with UV/Ozone. Mostly done on hydrophobic polymers but also on metals to improve adhesive bonding. Examples include a wide variety of thermoplastic and thermoset materials such as polypropylene (PP) polyethylene (PE), Carbon Fibre Reinforced Polymers (CFRPs), as well as rubbers,

6.2 Historical Development of UV/Ozone Surface Treatment

As early as 1972 Vig and LeBus described cleaning of silicon surfaces and stripping of photoresist by UV-light in combination with ozone gas generated by a single source for electronic applications [16]. The same approach was used by Zafonte and Chiu for the removal of organics and photoresist

residues on silicon wafers during production [18], or by Tabe for the removal of carbon from silicon wafers [19].

UV/Ozone treatment has been applied for the surface modification of thermoplastic screening systems based on microarray techniques which play a vital role in the fast advances of medical diagnostics as a part of life sciences [20]. Another researched application was the surface oxidation of batches of natural wool fibres, which appeared to cause a reaction of the proteinaceous carbon, leading to an increase of carbonyl functionality [21]. Other applications are the adhesion improvement of carbon fibres and carbon nanotubes to the matrix material leading to improved mechanical performance [22, 23]. UV/Ozone treatment was also applied on thin film solar cell surfaces to improve the wettability of the ink and therefore the surface coverage prior to inkjet printing by an indium-thiourea (In_2S_3) compound dissolved in a mixture of water and ethanol [24]. The use of low-pressure mercury UV-lamps as a direct source of germicidal disinfection is widespread, and can be found as a disinfection technique for public spas, hot tubs, waste or drinking water [25, 26] and also in the germicidal disinfection of recirculated air streams and surfaces [27]. Specific UV-lamps are known (and used) effectively for the photochemical generation of ozone gas, as the absorption of UV radiation by oxygen has a maximum efficiency at approximately 160 nm [28], which is about 15 nm below the lowest wavelength of the mercury spectrum.

6.3 Parameters Controlling the UV/Ozone Surface Treatment Process

6.3.1 Ultraviolet (UV) Light Spectrum

UV-light is a small fraction of wavelengths that belong to the visible part of the electromagnetic spectrum which runs from X-rays (wavelength 10^{-2}m), visible light (380 – 750 nm) (1nm = 10^{-9}m), radio waves up to television transmission wavelengths (10 – 10^{-1}m) [29].

The UV spectrum is divided into three main parts:

- UV-A: 400 – 315 nm;
- UV-B: 315 – 280 nm;
- UV-C: 280 – 100 nm (and lower) wavelengths.

The UV-A part of the light spectrum is part of the sunlight that drives photochemical processes, while UV-C is dangerous for human beings, as

it is strongly absorbed by deoxyribonucleic acid (DNA) and ribonucleic acid (RNA) and as a result can cause skin cancer, and for this reason it is effective in germicidal disinfection processes [30].

6.3.2 UV-Light Generation

There are several types of UV- light sources such as:

- Fluorescent lamps: Mercury-vapour filled low, medium and high pressure fluorescent discharge lamps. An electric current in the gas excites mercury-vapour, which produces shortwave ultraviolet light. Typically 30 to 40% of the electrical power input is transferred into UV-light. The ozone generating UV-C lamps have an emission spectrum with a radiance of 90 to 98% at two wavelengths, with the main resonance line at 253.7 nm, which is close to maximum of the germicidal curve, and a much smaller one at 184.9 nm (Figure 6.1). These low-pressure mercury arc discharge types (10^{-3} Torr) are often used as a disinfection light source [31] but are also found to be well suited for pre-treating polymer surfaces. The optimum operating temperature of fluorescent lamps when operated in the open is 20 – 30 °C should not reach more than 40 °C. A rapid growth in light technology showed the development of amalgam fluorescent lamps, which use hard alloys of mercury with metals that allow

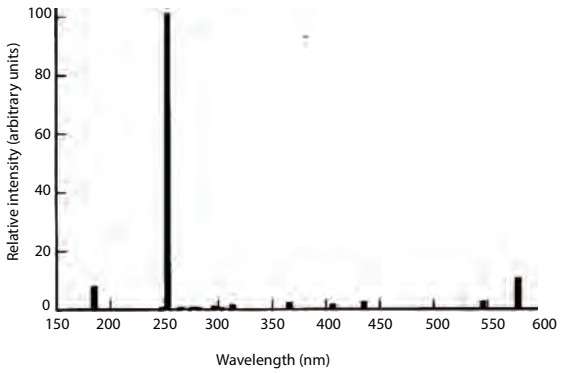

Figure 6.1 Low pressure mercury lamp UV-C spectral energy distribution [14].

higher light output. This implies, however, a slightly longer warm-up time before use [32].
Besides this, the user should be aware of the limited lifetime of fluorescent UV-lamps, as their housing is made of different quartz materials. Normal window glass allows mainly UV-A and visible light [33], while synthetic and natural quartz glass housings are available for germicidal disinfection purposes and added ozone production, respectively. However, the transparency of these quartz housings shows the steepest radiation reduction at 253.7 nm in the first 100 hours. The overall radiation power depreciation at 253.7 nm is about 25% after 8000 hours [34].

- Excimer lamps: These are Radiofrequency (RF) electric discharge light sources, which radiate quasi-monochromatic light, operating over a wide range of narrow emission bands with wavelengths from 351 down to 108 nm. Light is generated by a silent discharge between two electrodes. Due to an internal cooling system, the generated light is considered as "cold" and typically shows a high power spectral density of UV radiation [35].
- Light Emitting Diodes (LEDs): The electrical efficiency of LEDs is far higher than those of all other light generating sources, and the output shows narrow bandwidths down or near to 255 nm, good enough to be applied in germicidal technology [36].

6.3.3 UV-Light Sources Used

All presented data in this chapter were mainly generated using different types of low pressure mercury vapour fluorescent lamps and setups. The basic design of these instruments (unless stated otherwise) is shown in Figure 6.2. It shows an in-house built closed cabinet covered by aluminium sheets on the inside for improved light reflection, and it contained any of 3 types of ozone generating UV-C lamps:

- Three 4 W low pressure mercury lamps, type HUV5, Philips Lighting, The Netherlands (Section 6.3.5);
- One 80 W low pressure mercury lamp type NNIQ 120, Heraeus Noblelight GmbH, Germany (Sections 6.3.6–6.3.8, 6.4.5, 6.3.3, 6.3.5, 6.3.6, 6.6.4);

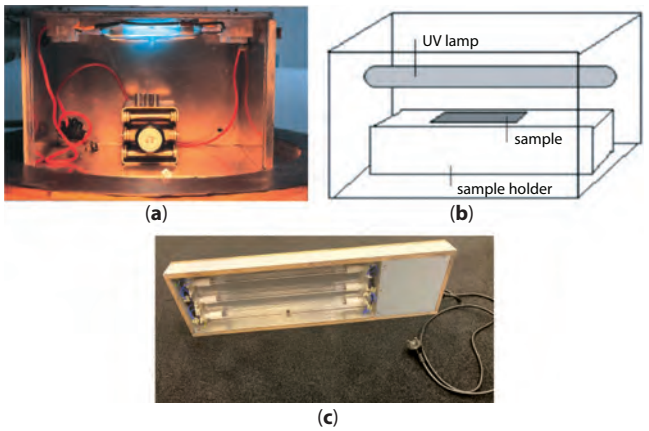

Figure 6.2 (a) Photograph of an early UV/Ozone chamber used for the experiments described in section 6.3.3 with three stainless steel cylindrical samples on a mechanical lift [14]. (b) schematic representation of the UV/Ozone exposure chamber used for the described measurements. (c) photograph of one of the most often used setups of three combined low pressure mercury lamps for the discussed experiments.

- Three 30 W low pressure mercury lamps type UVN 30 with a spacing of 50 mm between the lamp centres, and a radiation flux at 253.7 nm of 10 W, measured after 100 hours [34], UV-Technik Speziallampen GmbH, Germany, (Sections 6.5.1, 6.5.6, 6.6.2, 6.3.1, 6.3.2, 6.3.4, 6.3.7-6.3.11).

The specimens were always placed at a distance of max. 20 mm from the UV lamp (unless stated otherwise). All tests were performed at laboratory conditions.

Some of the experiments described below were performed either with an Excimer 222 nm or an Excimer 172 nm monochromatic light source. Just as lasers they have proved viable in the modification of polymer surfaces such as fluorocarbons [35]. The Excimer prototype light sources used in the described experiments below were supplied by Heraeus Noblelight GmbH, Germany. This first-generation Excimers had an efficiency of 10% of the electrical power input, which equals 1.5 W/cm lamp length at 172 nm. In comparison, a low-pressure mercury UV-source has an electrical input power of 2 W/cm and with its efficiency of 30 - 40% it generates about 0.06 W/cm at 184.9 nm. The light-photon bombardment per unit surface area of the Excimer lamp thus is about 25 times higher.

The cabinet of the Excimer 172 nm was filled with laboratory air with a pressure reduction to an "estimated optimum" of 1 mbar, in order to reduce the full absorption of the UV-light by oxygen gas and moisture.

6.3.4 Photochemical Ozone Generation

Ozone gas is well known as the protective layer for life on Earth, as it strongly absorbs shortwave sunlight in a wide range of lower wavelengths (Figure 6.3) and as such prevents most of it from reaching the Earth's surface, preventing destruction of animal and plant DNA [37]. However, on earth Ozone (O_3) can also be generated by exposing oxygen gas (O_2) to shortwave UV-light below 240 nm. This means that all three discussed UV- sources (low pressure mercury, Excimer 172 nm (Xe gas fill) and Excimer 222 nm (KrCl gas fill) will generate ozone from oxygen gas.

However, the ozone generation varies depending on the design and lamp power from 6-12 g/kWh^{-1} for low pressure mercury lamps to 60-100 g/kWh^{-1} for the 172 nm Xenon Excimers. For a 40 W low pressure mercury lamp the amount of ozone generated would be around 0.3-0.5 gh^{-1}. Hence, near to the lamp the concentration might be significantly higher [28].

Ozone is an unstable molecule with a "half-life" of about 705 minutes (24 °C, 45% RH) up to 5 days (based on the literature) [e.g. 28]. It has a strong oxidizing nature, a typical smell and is dangerous to human beings with a Maximum Allowable Concentration (MAC) value of 0.1-0.3 Parts

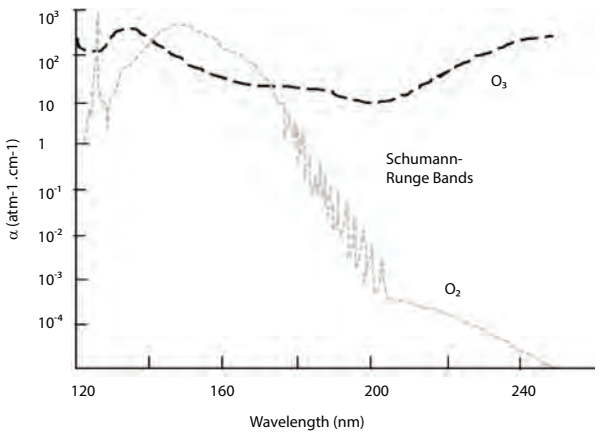

Figure 6.3 Wavelength dependent absorption (α) of oxygen and ozone gas. Please note the exponential vertical scale.

Per Million (PPM) [16, 34, 38–40]. However, the values for maximum allowed concentration and exposure time differ internationally.

6.3.5 Relation between Ozone Generation and UV-Source Power

The photochemical ozone generation by two HUV 4 W low pressure mercury lamps (Philips Lighting, The Netherlands) with essentially both 184.9 and 253.7 nm (Figure 6.1) was measured by an ozone analyser (model 8810, Monito Labs, Envico, Zoeterwoude, The Netherlands) as a function of medical oxygen gas input in a laboratory built UV/Ozone cabinet of 1.5 litres (Figure 6.2a). The results showed that an increase in the source power as well as an increase in oxygen gas flow leads (asymptotically) to an increased ozone concentration (Figure 6.4). The lower the UV-source power, the faster the maximum ozone concentration is obtained, though at a lower concentration than would have been obtained at a higher power [14].

Note that the light absorption of both oxygen and ozone gas covers the whole UV-C spectrum (Figure 6.3). This means that the breakdown of ozone into oxygen by the absorption of UV-light has to be taken into account. The calculated relative light intensity as a function of the distance from the UV-source is shown in Figures 6.5a and b. The UV-light is strongly absorbed by molecular oxygen below roughly 200 nm (Figure 6.5a) and by ozone molecules above 200 nm (Figure 6.5b). As a result, these graphs show the importance of the minimal distance between the

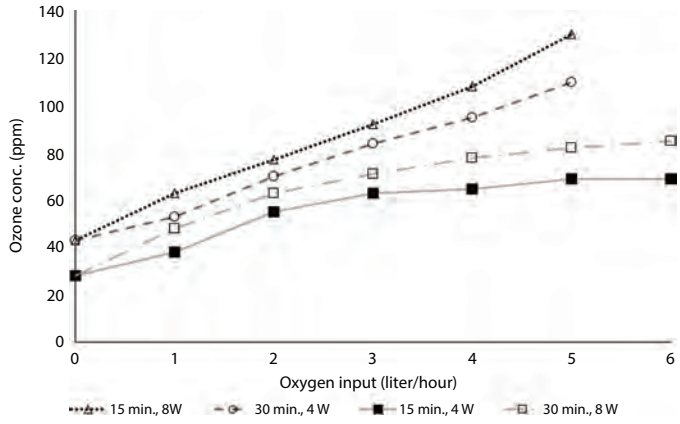

Figure 6.4 Ozone concentration in a UV/Ozone exposure chamber (Figure 6.2a) containing two 4 W UV-C light sources as a function of the oxygen input flow and the UV-source power.

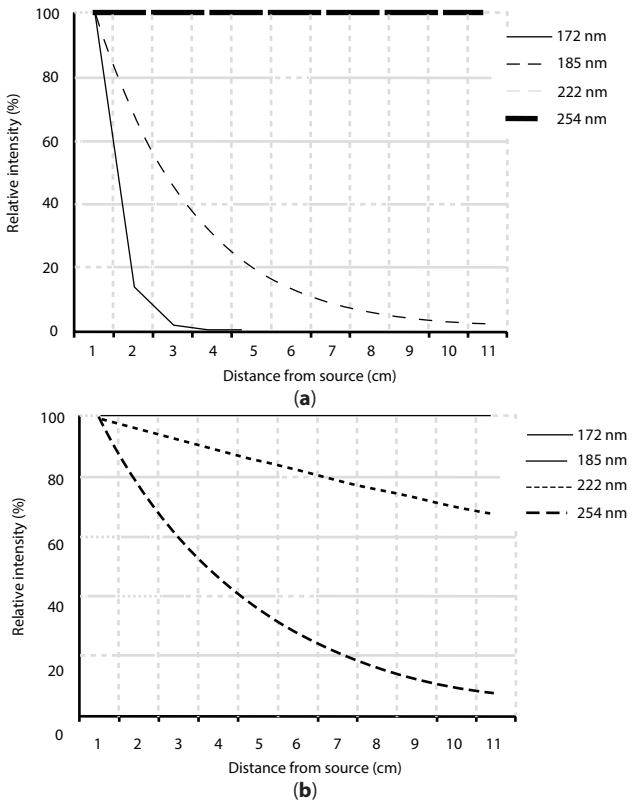

Figure 6.5 Relative intensity of UV-light at 172, 185, 222 and 254 nm as a function of distance from the source due to absorption of oxygen (a) and ozone gas (b). (a) UV-light absorption by oxygen. (b) UV-light absorption by ozone.

UV-source (max. around 2 cm, Figure 6.5a), or a gas pressure reduction is needed, when an Excimer 172 nm is used. The same graph shows that 222 nm and 253.7 nm are hardly affected, and thus the resulting data are overlapping. A similar phenomenon occurs with the absorption of ozone gas molecules (Figure 6.5b): the UV-light at 253.7 nm has the highest absorption of ozone gas from all investigated wavelengths, while 172 nm and 184.9 nm are hardly affected by ozone and are, as a result, overlapping.

6.3.6 Temperature during UV/Ozone Treatment on Polyolefin Surfaces

The temperature in both UV-exposure cabinets, the low-pressure mercury lamp and the Excimer 222 nm were measured (Figure 6.6), as this

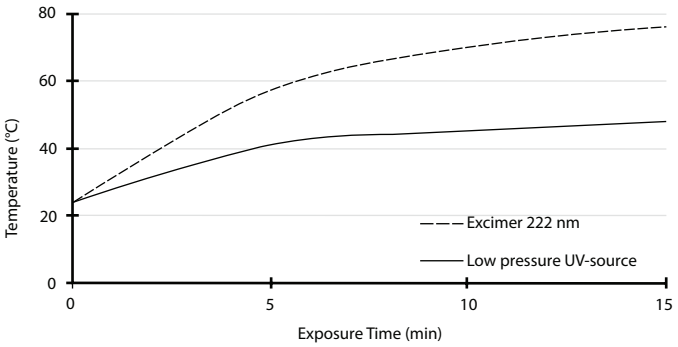

Figure 6.6 Typical sample temperatures as a function of treatment time on exposure to two different UV-sources.

temperature might influence the reaction velocity of the chemical processes, the lamp efficiency, as well as the stability of the sample materials. The measurements showed that the temperature of the low-pressure mercury lamp was rather stable and near the optimal performance temperature of fluorescence lamps of 40 °C, while the sample temperature during the surface treatment by the Excimer 222 nm was much higher, increasing with time and reaching over 70 °C after 15 minutes.

6.3.7 Influence of Wavelength(s) and Gas Fill on Polyolefin Surfaces

Polypropylene (PP) is a thermoplastic, partly crystalline, material that, like polyethylene (PE), belongs to the group of polyolefins [17] with rather similar properties, though it is slightly harder and more heat-resistant. Its non-polarity (hydrophobic nature) and low surface free energy of about 30 mJ/m^2 (Figures 6.7a, b) makes it difficult to bond without increasing its wetting performance [41, 42].

The surface free energy and bond strength were measured on pure Polypropylene samples (PP, Vink Kunststoffen, The Netherlands) in order to find the optimal combination of wavelengths and ozone gas for the surface activation. Three different types of UV-sources were used: a low-pressure mercury UV-lamp, an Excimer 172 nm and an Excimer 222 nm.

The treatment chamber of the Excimer 172 nm was filled (pressure: 1 mbar) with nitrogen, laboratory air, or laboratory air saturated with water. The surface free energy of the PP surface was measured by test inks (Arcotest, Mönsheim, Germany) as a function of the exposure time

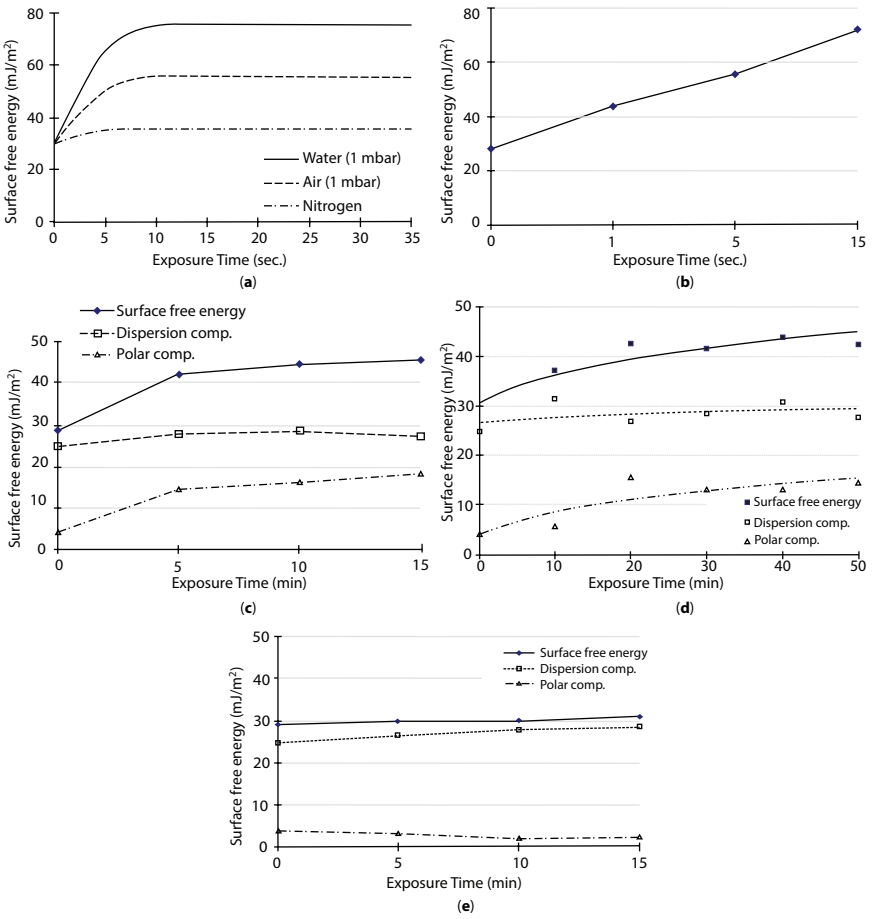

Figure 6.7 (a) Trend lines showing the surface free energy of PP as a result of exposure to the Excimer 172 nm in different gas atmospheres. (b) Surface free energy of PP exposed to the Excimer 172 nm as a function of exposure time. (c) Surface free energy of PE due to exposure to the (whole) spectrum of a low-pressure mercury UV-source. (d) The same as (c), but with a 185 nm UV-filter, and (e) the surface free energy on exposure to the Excimer 222 nm.

(Figure 6.7b). The surface free energy of the PP remained at the same low value when only nitrogen gas was present in the reaction chamber, meaning that no polar groups were generated on the surface. But introducing oxygen (laboratory air), with or without water, showed a strong increase of polar groups on the surface, which was the highest when water molecules were present. The water molecules tend to break apart into reactive radical species like OH* which can react with the polymer surface. Hence, these

experiments show that oxygen radicals need to be present for surface oxidation which are increased in the presence of water vapour.

Figures 6.7a and b show that exposure of PP to 172 nm resulted in a maximum surface free energy of 72 mJ/m^2 when exposed to moist air. This value clearly surpasses that obtained from the other two gas environments: just laboratory air and definitely that of nitrogen gas. Note that the activation time is in the order of seconds instead of minutes (like that of the low-pressure mercury source).

Further experiments to determine the effects of the combinations and separate UV wavelengths were carried out on pure polyethylene (PE, Vink Kunststoffen, The Netherlands). For the Excimer 222 nm and the low pressure mercury UV- source the surface oxidation was determined by water contact angle (*) measurements as a function of the exposure time.

(*) All contact angle measurements for wetting and surface free energy experiments were done at room temperature at a RH of 50% using either a KSV CAM 200 (Chem. Instruments, USA), or a Krüss G2 (Krüss, Germany) computer controlled drop shape analysis system with drop volumes of 3 - 5 µl. All reported data are averages over at least three droplets, placed at different positions on the specimens.

An Action Research Corporation (ARC) 01720 filter (peak wavelength of 184 nm, bandwidth 24 nm and a peak transmission of 24.8%) was placed 5 mm above the polymer surface to block all other wavelengths (thus ozone gas as generated by the UV-lamp could still reach the surface). This arrangement made it possible to measure the effect of just 184.9 nm together with ozone gas without exposing the polyethylene (PE) to 253.7 nm. As a result PE could be exposed to the low-pressure mercury lamp both with (Figure 6.7d) and without the 185 nm filter (Figure 6.7c). The results show an increase in the total surface free energy, independent of the filter used. This leads to the observation, that 184.9 nm plays a negligible direct role in the surface modification, though needed for the creation of the oxygen radicals which is in agreement with the results found by MacManus *et al.* [43].

However, as measured by test inks, the Excimer 172 nm (Figures 6.7a, b) showed the largest increase of surface free energy (during the shortest exposure time) for the three tested UV-sources, when used in a moist environment [44]. In contrast, the Excimer 222 nm hardly affected the surface free energy, and was unable to increase the surface polarity (Figure 6.7b). The effect is also visible when the same tests were done on PP instead of PE. The above measurements show the necessity of specific wavelengths in combination with ozone gas for a fast photo-oxidation process to create polar groups on the surface of the polymer.

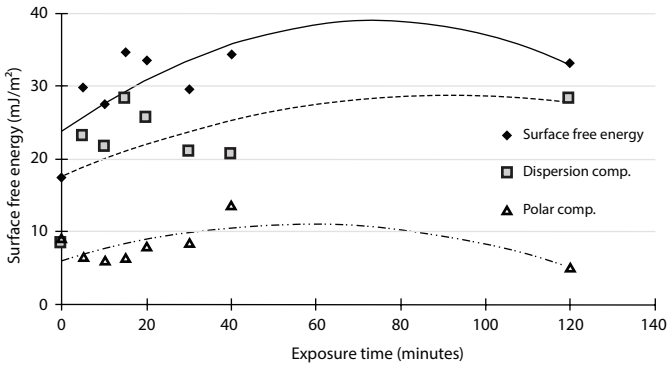

Figure 6.8 Measurements with added trend lines to show the course of a prolonged surface treatment by a low pressure mercury UV-source on the surface free energy of PP.

Figure 6.8 shows the occurrence of an optimum value of the surface free energy as a function of treatment time, though the highest adhesive bond strength appears to occur at a treatment time that is slightly less. Increasing the treatment time beyond the optimum value of the surface free energy will lead to an even further decrease of the adhesive bond strength, due to the creation of Low Molecular Weight Oxidized Molecules (LMWOMs) [45, 46].

6.3.8 Influence of Ozone Gas and UV-Light Spectrum on Polymer Surface Wetting

The influence of combinations of the UV-light spectrum and ozone gas concentration on the wetting of polymer surfaces was investigated to give a better insight into the relation between these two process variables to improve surface wetting.

The data shown below are the experimental results of a low-pressure UV-source with a transmission starting at 253.7 nm from a TUV-glass lamp sleeve instead of a fused quartz sleeve as used in all other discussed experiments in this chapter. Test samples were made of pure polypropylene (PP) (Vink Kunststoffen, The Netherlands) and only pre-cleaned with ethanol as a reference before exposure, shown as (254 nm) 0 min. in Figure 6.9.

The influence of the ozone concentration during the exposure was already found by some researchers [14, 16, 17, 47], though no experiments have been reported where the relations between the generated

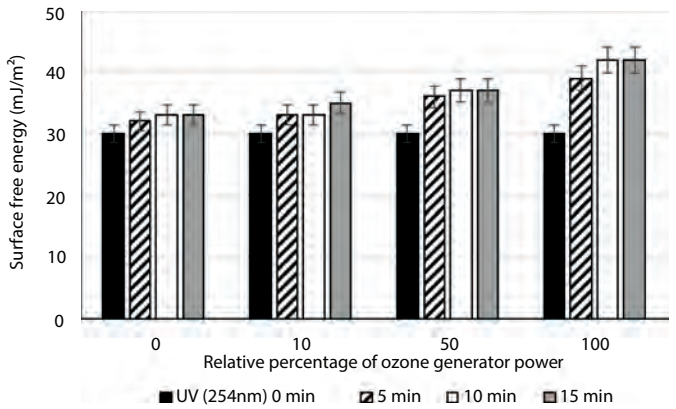

Figure 6.9 Surface free energy of PP measured by test inks. Pre-cleaned by ethanol as a function of various UV-light (>253.7 nm) exposure times and ozone concentrations.

separate wavelengths and the ozone concentration are shown. The ozone in this experiment was generated by an Ozone Technology OT20 (Ozone Technic, Turkey) ozone generator (20 g/m^3 at 100% power range). The surface free energy test results on the PP samples were determined by test inks (Arcotest, Mönsheim, Germany).

Exposure to ozone gas alone did not show any increase of the surface free energy within the standard deviation (STD). Though increasing the ozone concentration together with a longer UV exposure time showed a small (but a clear) increase of the average surface free energy.

The above results show that the efficiency of surface activation by ozone and/or 253.7 nm without 184.9 nm is negligible and low. The surface free energy due to 253.7 nm only increased when the ozone concentration was increased, but it was still far lower than when the combined wavelengths (183.9 and 253.7 nm) were generated by a single low pressure mercury UV/Ozone lamp (Figure 6.8).

6.3.9 Main Process Variables: Overview

The number of variables related to the UV/Ozone cleaning and surface functionalisation process are limited. The main ones are:

- The type, power and age of the UV- light source (generated wavelengths and intensities);

- The distance between the UV- light source and the treated object (the efficiency decreases exponentially with the distance) [14];
- The ozone concentration.
- The temperature of the process environment (influencing the reaction rate, the efficiency of the UV-light source, as well as the stability of the ozone gas);
- The relative humidity (RH) [48]

6.4 Surface Changes of Polymeric Materials by UV/Ozone Treatment

6.4.1 Polymer Bonds

The bond energies of several atomic bonds which are of importance during the UV/Ozone process are listed in Table 6.2. For comparison, the photon energies at different wavelengths are given in Table 6.3.

The generated photons from UV-light of e.g. 253.7 nm are clearly much less energetic than those from 172 and 184.9 nm but still gives them the ability to generate chain scissions in the carbon-carbon polymer bonds with bonding energies as shown in Table 6.2, because the photon energy (Table 6.3) should at least be equal to the bond energy (Table 6.2) to break these bonds.

Table 6.2 Bond energies of several atomic bonds of importance during the UV/Ozone process.

Type	H_2C-H	HO-H	HOO-H	OO-H	H_3C-CH_3	O=C=O	N≡N	O=O
Bond energy (J)	6.6 E-19	7.5 E-19	5.6 E-19	5.6 E-19	5.6 E-19	8.1 E-19	14.3 E-19	7.6 E-19
Bond energy (kJ/mole)	438	498	369	374	376	532	945	498

Table 6.3 Relevant spectral lines during the UV/Ozone process in relation to the transmitted energy/tube length and the number of photons/cm^2, together with their photon energies.

Wavelength (nm)	Energy/cm tube length	No. of photons/ cm^2 per second	Photon energy (J)	Photon energy (eV)
254	2.7 W *(low pressure UV-lamp)*	3 E18	7.7 E-19	4.8
222	12.5 W (*first generation Excimer)*	14 E18	8.9 E-19	5.6
185	0.3 W *(low pressure UV-lamp)*	3 E18	10 E-19	6.8
172	50 W/cm *(new generation Excimer)*	41 E18	12 E-19	7.2

6.4.2 Surface Cleaning by UV/Ozone: Increasing Hydrophilicity and Surface Free Energy

The lower wavelength of the mercury spectrum which is transmitted by a low pressure mercury lamp with a natural quartz housing is 184.9 nm (with an energy of 155 kcal/mol) and is thus capable to break various polymer bonds like: H_3C-H (102 kcal/mol), CH_{2-}CH-H (105 kcal/mol) and CH_3-CH_3 (84 kcal/mol). This results in the phenomenon that during exposure to UV/Ozone from a low pressure mercury UV-source, the polymer chains and organic contaminant molecular bonds are broken (chain scissions) by the photochemical process of the highly energetic light quanta of 253.7 nm and 184.9 nm [25, 26].

Besides this, a kind of plasma arises, where reactive oxygen radicals O (^{3}P) from oxygen molecules (O_2), as shown schematically in Figure 6.10a, might react with (unstable) ozone molecules (O_3), which can be dissociated (photo-decomposed) into molecular oxygen (O_2) and an oxygen radical O(^{1}D) by 253.7 nm.

This radical O(^{1}D) is a reactive atomic species, which, as a result, can oxidize the surface and create functional polar surface groups such as OH, OOH, and C=O, which increase the wettability [15, 48]. Meanwhile,

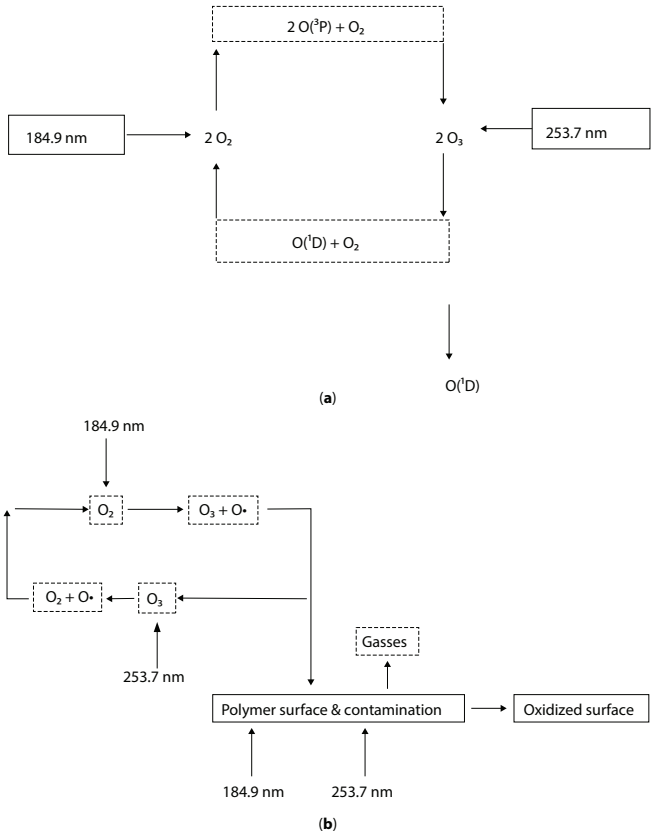

Figure 6.10 Simplified schematic models of (a) ozone generation and destruction by low pressure mercury UV-sources and (b) the UV/Ozone surface cleaning and activation process.

traces of oxidized surface contaminants leave the process in a volatile state (Figure 6.10b) [15, 16].

This continuous process of forming and destroying ozone gas and the generation of oxygen radicals is in fact a kind of reactive cold plasma. As a result, polymers are oxidized in this aggressive environment of UVC-light, ozone gas and oxygen radicals. On a nano-scale polymer surfaces will either become nano-roughened [49] or nano-polished [45], depending on the type of polymer. Very thin layers of organic contamination will thus be eroded, and will finally disappear from the surface.

In literature only few authors like Vig and LeBus [16] investigated the importance of the combination of UV-light and ozone gas on the cleaning performance (the decomposition of organic contaminants) on materials

such as metals and silicon wafers, which increases the surface wetting by hydrophilic liquids like water.

Indeed, UV/Ozone proved to be an excellent cleaning method for the thorough removal of the last traces of organic contaminants from metal surfaces [19]. Furthermore, previous research showed that UV/Ozone treatment improved the (initial) adhesive bond strength and durability between a metal and epoxy, especially when used in combination with sol-gel and water-based primers [19, 20, 45, 50, 51].

As already mentioned above, UV/Ozone was found to be capable of removing the last traces of organic surface contamination and is very often able to increase the hydrophilicity of the surface as a result of surface oxidation which is the minimum requirement for good wetting. This was the precursor for high quality initial and durable adhesive bonding of many polymers.

UV/Ozone treatment of polymers for a combined cleaning and surface functionalisation by low pressure UV-sources generally takes between 5 and 15 minutes. Depending on the polymer material and process variables such as the power of the UV-source and its distance from the substrate, it often results in an increased polarity and an increased wettability of polar liquids [52]. This is a large advantage for the interfacial (or adhesion) strength of an adhesive, sealant, coating, paint or printing ink as well as adhesion of metallized polymers and of micro-organisms or cells. The adhesive bond strength of polymer surfaces is often found to increase compared to the initial (untreated) value as a result of the larger number of polar and non-polar interactions resulting in a larger density of near-surface cross-links [53]. Hence, the photonic degradation and oxidation process strengthens the outermost surface layer and increases the interaction necessary for improved adhesion. Besides, the durability of the adhesive bond in harsh environmental conditions often increases as a result of these increased molecular interactions across the interface.

6.4.3 Photo-Degradation: Surface Roughness and Morphology Changes

Light that strikes a plastic surface may either be reflected from the surface or absorbed. The last process may remove a hydrogen atom from the polymer forming an unstable radical which starts the photo-degradation process [54]. As a result, plastic weathering involves changes in the physical, mechanical, and chemical properties of polymers, particularly at the surface, leading to changes in gloss, morphology and roughness [55, 56]. Thus it is essential to know the physical state of the polymer and its fundamental

mechanism of oxidative degradation in the absence of UV-light in order to understand what is happening in the presence of ultraviolet radiation and oxygen [57].

6.4.4 UV-Light Treatment Depth in Polymer Surfaces

An important criterion is the depth to which the surface is oxidized. Preferably, only the outermost layer is oxidized, thus keeping its bulk mechanical properties unchanged. Experiments on polypropylene (PP) and poly(ethylene terephthalate) (PET) have shown that the oxidation depth of flame treatment is the lowest, followed by corona and vacuum plasma. UV/Ozone treatment has a far deeper penetration depth [58]. Atmospheric plasma is somewhat less efficient and will penetrate less deep into the bulk mass than the vacuum plasma type, thus taking slightly longer to obtain the same result as the vacuum plasma surface treatment [59].

UV/Ozone treatment is found to penetrate relatively deep into the bulk of the polymer in comparison with the more familiar surface treatments such as flame, corona and plasma treatments on e.g. PP and PET films. Hill and co-workers argue that the surface modification by a UV/Ozone treatment as well as by ozone treatment alone extends quite deeply (1 μm), well beyond a few monolayers. This should be considerably less for corona- or plasma-treated samples. Flame treatment appears to be the "shallowest" meaning that the oxygen incorporated by the treatment is mostly concentrated near the outermost layer of the polymer surface (see also sections 6.5.3 and 6.5.4) [49].

6.4.5 Surface Relaxation of HDPE

The surface oxidation of a polymer as a result of a physical treatment will (partly) disappear as a function of time due to reorientation and migration of the (functional) groups on the surface. The three graphs of Figure 6.11 representing measurements on HDPE show that the decrease in surface wetting by water was found to be dependent on the surface treatment method and was found to be far higher after the atmospheric plasma (**) than after either corona (***) or UV/Ozone treatment.

(**) All atmospheric plasma experiments were done in a laboratory environment using a Tigres Plasma-Blaster (Tigres GmbH, Rellingen, Germany) equipped with three separate plasma guns. (300 W power supply, gas pressure 4 bar, distance 20 mm from the object).

(***) All corona experiments were done in a laboratory environment using a TIGRES Corona instrument (Tigres GmbH, Rellingen, Germany) equipped

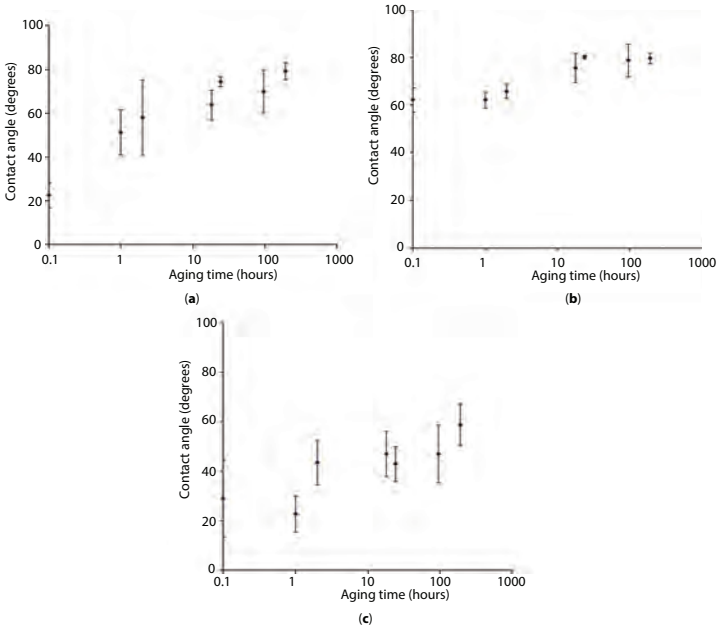

Figure 6.11 Aging of a HDPE surface determined by water contact angle as a function of exposure time in a laboratory environment after treatment by: Corona (a), UV/Ozone (b), and atmospheric plasma (c).

with a 300 W power supply, gas pressure: 4 bar, torch distance 10 mm from the object.

All oxidized polymer surfaces will show this effect, depending on a number of factors such as crystallinity, purity and molecular weight. Higher crystallinity (HDPE: 60% - 80%) will increase the stiffness of the polymer chains, leading to a less likely or slower reorganisation of the functional groups on the surface to return to the bulk. Especially, increased crosslinking will increase the lifetime of functionalities at the surface. Reorganization to the bulk mainly takes place in the amorphous part of the polymer and by the low molecular weight oxidized molecules, which have more freedom of movement.

Kim and co-workers found that the surface relaxation is also dependent on the type of gas (mixture) used. Plasma treatment was found to lead to an optimal balance between a high oxidation level and survival time of the oxidized groups at the surface at a gas mixture of argon and oxygen in the ratio 9:1 due to an increased amount of crosslinks and thus stiffness of the polymer chains [60].

6.5 Surface Analysis of UV/Ozone Treated Polymeric Surfaces

6.5.1 Scanning Electron Microscopy (SEM) on UV/Ozone Treated Carbon Fibre Reinforced Polymer (CFRP)

The measurable changes that UV/Ozone treatment might have on the surface properties and morphology of a polymer, and specifically CFRP, are discussed below in more detail. The CFRP used was a HexPly 8552 unidirectional prepreg with a toughened amine curing epoxy resin in combination with AS4 carbon fibres (Hexcel Composites, Duxford, UK).

SEM micrographs (instrument: JEOL JSM-7500F) were taken and are shown in Figures 6.12a-c, in order to discover if any changes in the surface morphology would become visible as a result of the UV/Ozone surface treatment. A single CFRP sample (sized 2.5 x 2.5 cm, with a thickness of 10 plies) was subjected to various UV/Ozone exposures, using a folded aluminium foil mask, and images were made (Figures 6.12a-c).

The SEM micrographs revealed no clear change in the surface morphology, as expected, and thus Atomic Force Microscopy (AFM) scans with a far higher resolution were made (section 6.5.2).

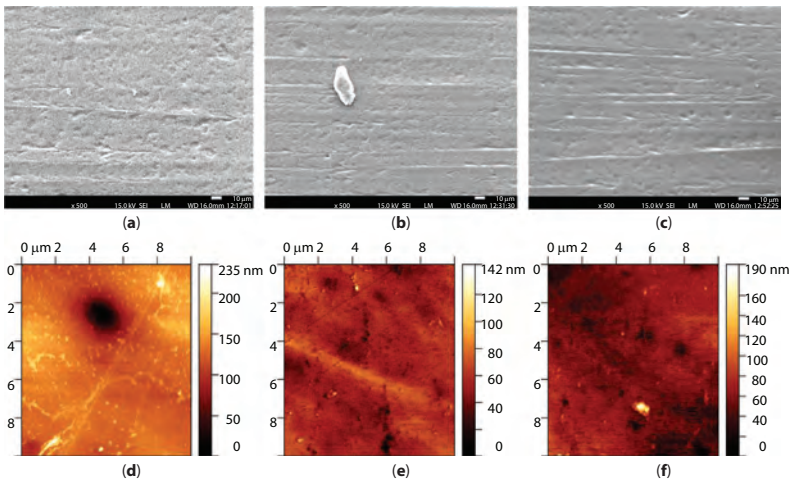

Figure 6.12 SEM (a, b, c) and AFM (d, e, f) micrographs of (a, d) the CFRP surface acetone cleaned only (reference), (b, e) after 6 minutes of UV/Ozone (a dust particle is visible in the SEM micrograph) and (c, f) 10 minutes of UV/Ozone treatment. a: (Acetone cleaned (reference), 500x, b: UV/Ozone 6 min., 500x, c: UV/Ozone 10 min., 500x.

6.5.2 Atomic Force Microscopy (AFM) on UV/Ozone Treated CFRP

AFM imaging was done to measure the morphology of the surface on a nanoscale level by a Dimension Edge Scanning Probe Microscope (Bruker, Germany) with a silicon probe TESPA (Bruker). The sample for the AFM measurements was 20 x 25 mm (with 10 plies thickness). It was visually divided into sections made by an Edding 780 silver paint marker pencil, and during the surface treatment partly covered with a mask of folded aluminium foil to allow for 0, 6 and 10 minutes of UV/Ozone treatments on a single sample. Each presented value is the result of at least three measurements.

The AFM micrographs are presented in Figures 6.12d-f and the test data can be found in Figure 6.13a/b, showing two of the CFRP surface parameters the root mean square roughness (R_q) and the arithmetical mean height (R_a). Each value was averaged from three measurements on 10 x 10 µm scanned surfaces.

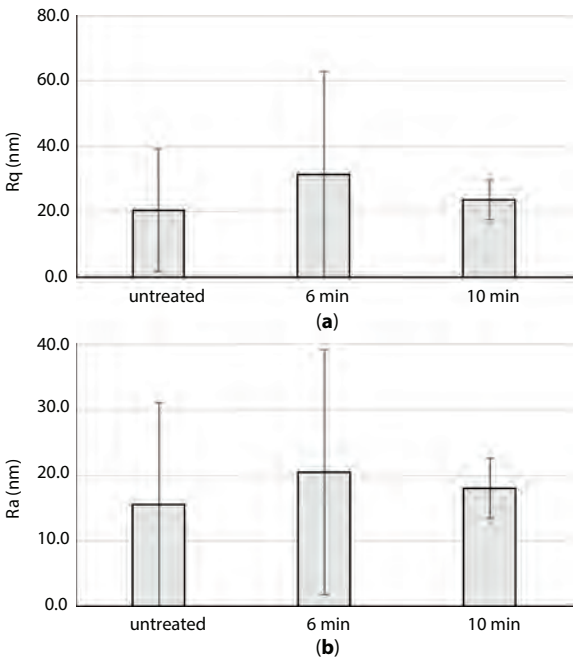

Figure 6.13 Averaged AFM data, showing: (a) The root mean square average height (Rq,) and (b) the arithmetical mean height (Ra) of the CFRP surface after acetone cleaned only ("untreated") as well as after 6 and 10 minutes of UV/Ozone treatment.

Neither (SEM) nor AFM scans showed any convincing evidence for a change in surface roughness of the CFRP as a function of UV/Ozone exposure time up to 10 minutes. These results are in contrast to the reported "less structured"/"smoothed" appearance of the same material as a result of a treatment by vacuum UV that Arikan *et al*. had found [45], possibly as a result of the large standard deviation in our AFM data.

6.5.3 X-Ray Photoelectron Spectroscopy (XPS) on UV/Ozone Treated CFRP

Three CFRP samples (sized: 50 x 30 mm and 10 plies thickness) were treated and analysed within 4 hours to observe the surface composition after a 7 minutes UV/Ozone treatment. For this purpose, a K-Alpha X-ray photoelectron spectrometer (XPS) (Thermo Fisher, The Netherlands) was employed at ambient temperature using an Al Kα X-ray source. The cathode was set to 12 kV and the beam current to 3 mA, leading to a nominal spot size of 400 μm^2. The spectra were evaluated with Avantage software (version 5.9922) of Thermo Fisher Scientific. At the beginning, the satellite peak subtraction was performed. The background intensity of the spectra was described with the Shirley method [61–64]. Next, the positions of the photoelectron spectral lines were determined. The charging up of the specimens was corrected by adopting a value of 284.8 ± 0.1 eV for the adventitious C 1s binding energy [64, 65]. The surface composition was then calculated from the peak areas of the identified elements, and the results are shown in Figure 6.14.

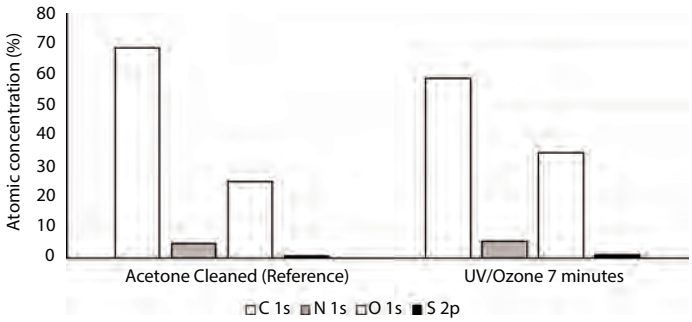

Figure 6.14 XPS data showing atomic concentration percentages of the elements carbon, nitrogen, oxygen and sulphur of the CFRP before and after surface treatment by UV/Ozone.

The O 1s/C 1s ratio increased from 0.37 to 0.52 as a result of the 7 minutes UV/Ozone treatment, clearly indicating an increased oxygen content at the CFRP surface. The XPS results thus showed an increased amount of oxygen on the surface of the UV/O_3 treated sample compared to the non-treated one due to oxidation. Washing the 7 minutes UV/Ozone exposed surface with acetone reduced the O/C value to 0.42 which was in line with expectation [45]. Etching of the above sample surfaces in the XPS instrument to a depth of 2 nm and 4 nm showed a strongly reduced oxygen content with O/C values less than 0.1, independent of the washing procedure. Hence, the oxygen content at this depth was far less than would be expected, based on the results obtained from other researchers [e.g. 45, 65].

6.5.4 Attenuated Total Reflection Fourier Transform Infrared Spectroscopy (ATR-FTIR) Investigation on UV/Ozone Treated CFRP

The change in surface oxidation of the CFRP due to exposure to a low pressure mercury UV-source and ozone gas was studied by FTIR, as this method detects changes in the polymer far deeper into the bulk than XPS (respectively: 1000 – 5000 nm and 2 - 5 nm) [66, 67].

Making use of a mask of aluminium foil, different exposure times could be obtained on a single sample sized 50 x 35 mm. To take into account any surface heterogeneity, a minimum of three spectra in different areas were recorded per sample and analysed on a Perkin Elmer Spectrum 100 FTIR spectrometer equipped with a universal attenuated total reflectance (ATR) ZnSe crystal sample accessory. Data were collected from 16 scans with a resolution of 4 cm^{-1} and are presented in Figure 6.15. No notable changes

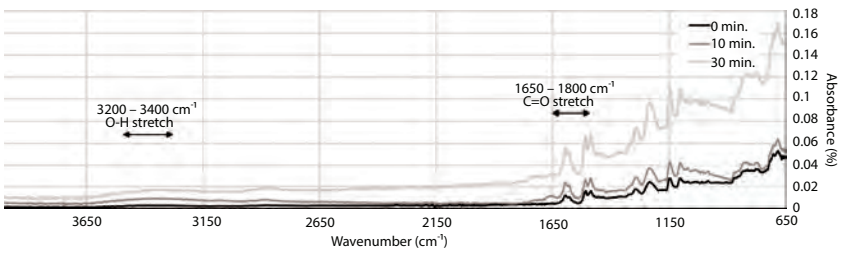

Figure 6.15 ATR-FTIR absorption spectra of CFRP surfaces at three stages of surface activation. The reference sample (0 min.) was acetone cleaned only, after which the sample was treated by UV/Ozone for 10 and 30 minutes.

were observed, therefore the ATR-FTIR spectra were not normalized, and only one spectrum for each measurement was chosen for representation.

The main changes in the chemical composition as a result of the increased UV/Ozone exposure time of the surface layer by oxidation were found by the formation of alcohol and carbonyl groups with strong stretching peaks between 3200 - 3400 and 1620 - 1870 cm^{-1} respectively as can be found in Figure 6.15. This increase in oxidation is in line with the results found by XPS (section 6.5.3) and the contact angle measurements (section 6.5.6. Furthermore, they are in agreement with those found by other researchers [46, 68].

Washing the samples with acetone directly after the UV/Ozone treatment did not show a measurable difference in the FTIR scan results. This implies that the washing procedure did not remove a measurable amount of some Low Molecular Weight Oxidized Molecules (LMWOMs) as an effect of chain scissions, from the surface to a depth of 0.5-2 μm, considering the scan depth of the infrared technique.

6.5.5 Optically Stimulated Electron Emission (OSEE) Investigation on UV/Ozone Treated CFRP

An accurate quantitative method to determine the surface properties is to make use of the photoelectric effect, described by Einstein who showed that electrons could be released from a surface when the absorbed energy of a photon exceeded the energy by which it was attracted [69]. The intensity of electrons emitted from such a surface is found to be related to the surface condition (e.g. the level of oxidation) and the amount (thickness) of contaminant layer present. The intensity of emitted electrons can be measured by an OSEE instrument, which exposes the surface to a narrow beam of UV- light and measures the number of emitted electrons as a result. This technique has found an important application in the adhesive bonding technology, especially in space related objects [70–72].

The OSEE instrument used was a SQM 200 surface quality monitor (Photo Emission Tech Inc., USA). When applied to a metal, the output signal increases when the surface becomes cleaner (less contaminated) e.g. after exposure to UV/Ozone. This effect is the result of an increasing stream of photoelectrons escaping from the surface. In contrast, when the same experiment is done on a CFRP surface, the output signal is strongly reduced as a function of the (UV/Ozone) treatment time, due to an increased static charge which prevents electrons from escaping the surface (Figure 6.16).

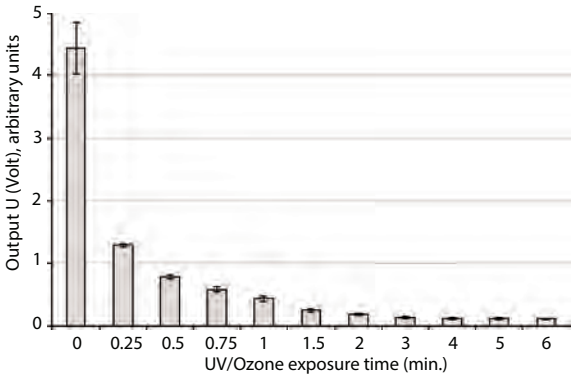

Figure 6.16 OSEE output voltage as a function of an incremental exposure time to UV/Ozone.

However, wiping/washing the surface with a polar liquid like acetone or water showed a (repeatable) steep rise of the OSEE initial signal as shown in Figure 6.17. The noticeable slight overall rise of the recovered OSEE signal is the result of a permanent change of the oxidation state and thus the electrical conductance of the CFRP surface.

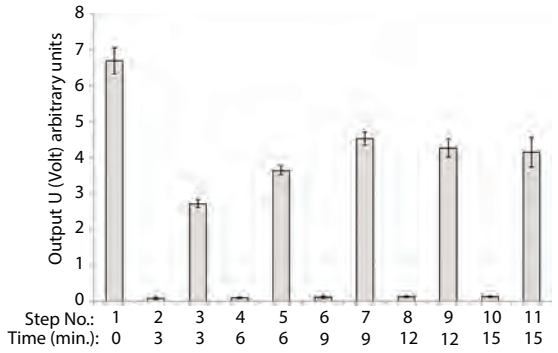

Figure 6.17 OSEE output voltage as a function of the UV/Ozone exposure time with an increment of 3 minutes/step and intermediate cleaning by acetone. Step1 is "As is" or no UV/Ozone exposure. Step 2 is after 3 minutes of UV/Ozone exposure. Step 3 is after 3 minutes UV/Ozone exposure including acetone wash. Step 4 is after 6 minutes UV/Ozone exposure, etc.

6.5.6 Contact Angle Measurements on UV/Ozone Treated CFRP

Contact angle measurements are sensitive to changes in surface chemistry and topography. Though the changes in topography as a result of the UV/Ozone treatment were not detected, as they were much smaller than 100 nm, as observed during the AFM measurements (section 6.5.2 [49, 73]). There are various approaches to determine surface free energies of polymers from the measured contact angles using appropriate test liquids, ranging from polar to dispersive liquids [74, 75]. The surface free energy values as a result of combined chemical and physical surface treatments (Figure 6.18) were calculated using the Owens and Wendt [76] approach from the static contact angle measurement data (droplet volume: 5 µl). They were measured on CFRP samples, sized 25 x 20 mm, with a range of liquids: water, formamide, diiodomethane, and glycerol.

The results of 10 minutes of UV/Ozone treatment showed a large increase of the polar component of the surface free energy compared to the just acetone cleaned surface. This is in agreement with the increase of the oxygen content of the surface as found with both XPS (section 6.5.3) and ATR- FTIR measurements (section 6.5.4).

Washing the samples with acetone directly after the UV/Ozone treatment did not show a measurable difference in the polar component of the total surface free energy. This implies that the washing procedure did not remove a measurable amount of polar groups generated by chain scissions during the UV/Ozone process, considering its treatment depth as 1 µm [58] and the scan depth of the ATR- FTIR technique as being only 0.5 – 1 nm [77].

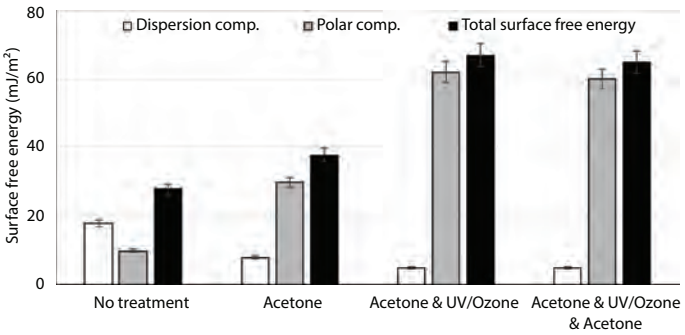

Figure 6.18 Surface free energy of CFRP together with its dispersion and polar components, when untreated, acetone cleaned only, acetone & 10 minutes UV/Ozone treated, as well as an added acetone cleaning step after the UV/ozone treatment.

Thus, while UV/Ozone treatment penetrates rather deep into the surface (about 1 μm), but contact angle measurements are sensitive to a depth of only 0.5-1 nm [77] and as a result far less sensitive to changes in the bulk mass. It might be concluded from the above results together with the mechanical measurement results (section 6.6.2.2) that in the uppermost layers only a few chain scissions occurred. These upper layers were thus rather uninfluenced by the washing procedure. In other words, the washed out LMWOMs must come from deeper polymer layers.

6.6 UV/Ozone Treatment of Polymers: Improved Wetting and Adhesion

6.6.1 Introduction: UV/Ozone Treatment of Polymers

The removal of photoresist polymers by UV-light and ozone gas (depolymerisation) was already described by Bolon and Kunz as early as 1972 [78], while its cleaning capability was extensively described by Vig and LeBus [16] in 1976. Still the application of UV/Ozone as a treatment for improved adhesion between polymer surfaces like polypropylene (PP) and adhesives was discussed by only a few researchers [43, 47]. On a molecular level, UV/Ozone treatment of polymers was discussed to explain the importance of high surface free energy (or increased surface wetting) for successful adhesive bonding e.g. by Mittal [52] or van der Leeden and Frens [79] and more extensively by Sham *et al.* for the functionalization of carbon nanotubes to improve the mechanical performance of an epoxy matrix by modifying the surface properties of nanoscale reinforcements such as nanotubes and graphite [80].

The application of this technique in the sealing of disposable thermoplastics for microfluidics was described in literature in 2009 [81]. Some researchers make use of added oxidizing agents during the UV/Ozone treatment such as chlorine dioxide (ClO_2) [82] or water which influences the atmosphere in the reaction chamber and as a result the ozone production [44].

The advantage of the UV/Ozone technique itself is that even in its most basic form it can be regarded as easy to use and highly reproducible for extremely high quality surface cleaning [44] to increase the surface polarity of hydrophobic polymers, including difficult-to-bond materials such as Ethylene-Propylene-Diene Monomer (EPDM) rubber or Ethylene-Vinyl-Acetate (EVA). The UV/Ozone technique was found by the authors to be capable of cleaning (metal and polymer) surfaces down to the very last

layers of contamination, even thin layers of Teflon© or silicone oil, metal drilling fluids or fingerprints. Hence, bringing environmentally-friendly high-quality cleaning for adhesive bonding within reach for commercial applications like e.g. in the shoe industry [6].

Several commercial UV/Ozone applications were explored [81, 83, 84] and sometimes even successfully commercialized like the cleaning of flat surfaces in laboratory environments. However, despite the technological successes, the technique never became as popular as corona or (atmospheric) plasma treatments in the field of commercially-based adhesion improvement. As high quality and reproducible surface treatment is becoming more and more important, especially with the increasing use of adhesive bonding in multi-material applications such as in the microelectronics, automotive, and aerospace industries where lightweight structures of Carbon Fibre Reinforced Polymers (CFRPs) are often adhesively bonded to metal parts such as titanium. UV/Ozone surface cleaning and activation was found to show valuable results as shown in various scientific publications [8, 9, 15, 17, 50, 70, 84].

6.6.2 UV/Ozone Treatment of Thermoset Materials

6.6.2.1 Introduction: UV/Ozone Treatment of CFRP

CFRP material combines high strength-to-weight ratio and stiffness which is a key issue in the aerospace industry in order to minimize the environmental impact of transportation. To achieve this, weight reduction of aircraft without compromising the structural integrity is a key issue. Within the scope of energy reduction falls the Hybrid Laminar Flow Control (HFLC) technology which reduces turbulence and increases laminar flow on the wing's skin of the leading edge. Effectively, this construction consists of a thin porous titanium grade CP 40 sheet which is adhesively bonded to a Carbon Fibre Reinforced Polymer (CFRP) inner structure (Figure 6.19) [85, 86].

The key to success of high quality durable adhesive bonding of such a structure strongly relies on the surface treatment of both substrates prior to the bonding process. Thus, it is crucial to promote the interfacial adhesion between the adherends and adhesive to obtain the highest bond strength and durability. With a properly selected surface treatment the adhesive bond should never fail at the adhesive-substrates interfaces, but cohesively within either the adhesive or adherends.

The surface treatments of both CFRP and titanium have been extensively studied, and are summarized in a review paper [87]. Various titanium

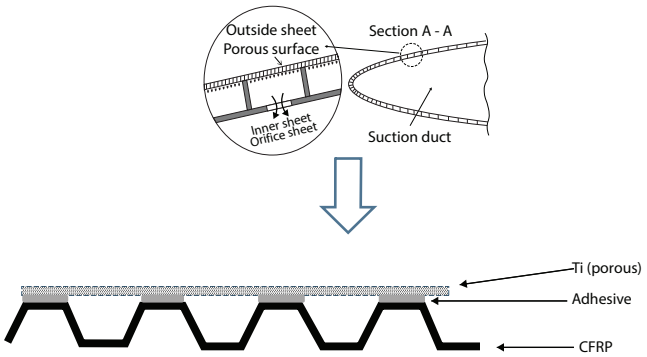

Figure 6.19 Sketch of Hybrid Laminar Flow Control (HFLC) (top) and a simplified 2D-version (bottom) showing adhesive bonding between titanium CP 40 top sheet and CFRP (inner structure of airplane wing) [86].

alloys have been used to study the effects of surface treatments. However, up to now, the application of the UV/Ozone technique as an integral part of the surface treatment for CFRP and titanium for structural adhesive bonding was reported by only a few researchers [e.g. 50, 68, 88].

The study of the UV/Ozone surface treatment of CFRP was extended to determine in more detail its effect on the epoxy matrix of the CFRP from a sub-micro to a macro-level. These sub-micro results showed that the observed changes occurred mainly on the outermost layer of the CFRP surface as a result of the UV/Ozone treatment. Additionally, mechanical test results are discussed when CFRP samples were tested in peel on a macro-scale (sections 6.6.2.2 and 6.6.2.3) and specifically when bonded to titanium CP 40 on a large test panel (resembling a realistic loading case of Figure 6.19) that was tested in mechanical fatigue loading (section 6.6.2.3).

6.6.2.2 Mechanical Tests on UV/Ozone Treated CFRP

Peel tests are the best mechanical test method to determine the weakest point of an adhesive bond [89]. Floating roller peel tests (ASTM D 3167-10) [90] are an excellent method to test adhesively bonded flexible to rigid multi-layer materials such as CFRP. The CFRP adherend was a laminate with a layup of either two plies (0°/90°) for the flexible part or ten plies (0°/ 90°/0°/90°/0°) for the rigid part, with a total thickness of approximately 0.27 mm and 1.55 mm respectively. During the fabrication process the surfaces of the laminates were in contact with a Fluorinated

Ethylene Propylene Copolymer release film (FEP Copolymer A 4000 clear red, Airtech Europe, Differdange, Luxembourg). The adhesive used in this study was the (red) knit supported carrier structural epoxy film AF163-2K designed for honeycomb and solid panel constructions, obtained from 3M, The Netherlands. The laminates were cleaned either with acetone or acetone with an added UV/Ozone treatment for 7 minutes.

The CFRP laminates were fabricated (sized 600 x 600 mm) and cured according to the specifications of the manufacturer in an autoclave (curing cycle of 180 °C for 120 minutes at 7 bar pressure). Specimens were cut by a diamond cutting wheel into smaller specimens sized: 255 x 25 and 305 x 25 mm for floating roller peel testing.

Mechanical test results were obtained on a Zwick 1455 test machine equipped with a 1kN load cell. The results (Figure 6.20) showed that the average peel strength values of these two groups of samples hardly differed. However, the acetone cleaned only samples show an adhesion (interfacial) failure while the UV/Ozone treated surfaces show an interlaminar (cohesive) failure of the CFRP, which indicates an increased adhesive bond strength across the interface. This is in line with previous observations by other researchers such as e.g Wang *et al.* [68] and Teixeira de Freitas *et al.* [91]. The change in failure type from adhesion failure between the adhesive and the CFRP to interlaminar failure is also in line with the above results, showing that an increased polarity of the CFRP surface layer results in stronger interactions across the CFRP-adhesive interface which were found to be, altogether, eventually stronger than those within the CFRP laminate [92–94].

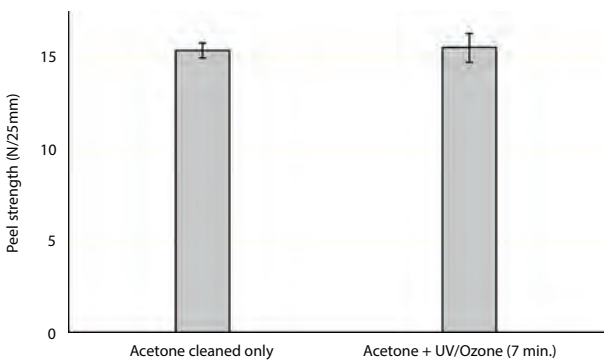

Figure 6.20 Floating roller peel test results for acetone cleaned only and those with a 7 minutes added UV/Ozone treatment of CFRP to CFRP bonded samples.

Washing the samples with acetone directly after the UV/Ozone treatment did not show a measurable difference in the mechanical test results (not shown in Figure 6.20) nor in the failure mode. This implies that the washing procedure and the removal of the LMWOM had no measurable effect on the bond strength as found in previous research [45].

6.6.2.3 Mechanical Fatigue Loading of UV/Ozone Treated CFRP

Two representative panels, based on the drawing shown in Figure 6.19, with a small artificially created defect between the titanium CP 40 sheet and one of the CFRP stringers, were subjected to in-plane cyclic loading. This loading involved an increasing in-plane compressive load, unloading, and then reloading to a higher load level until fracture occurred. The failure found was mostly adhesion failure at the titanium surface located in the vicinity of the artificial defect and cohesive failure within the adhesive layer further away from the artificially made defect [95]. This failure type is in line with previously found results discussed in section 6.6.2.2.

6.6.2.4 Adhesive Bonding of UV/Ozone Treated CFRP to Aluminium

UV/Ozone treatment was successfully applied for the surface preparation of aluminium bonded to CFRP when a study was done to replace Bisphenol A by an eco-epoxide adhesive synthesized from bio-renewable raw material (tannic acid—TA) and used for bonding lightweight materials (aluminium (Al) and a carbon fibre reinforced polymer (CFRP) as discussed by Tomić *et al.* [96].

6.6.2.5 UV/Ozone Treatment and Testing of Aerospace Primers

Generally, the surface treatment of primers before a top-coat layer is applied is done in a standard sequence that consists of degreasing (by solvent wipe), surface roughening to remove a thin and inactive surface layer and, again, a solvent wipe to remove dust particles [97]. Surface modification using UV/Ozone was explored by Haack *et al.* as an approach for robust inter-coat adhesion in multi-layered automotive coating systems. This treatment was used to reduce the variability in adhesion performance linked to changes in its surface chemistry resulting from migration of additives [98]. This approach was again investigated in the laboratories of the Adhesion Institute of the Delft University of Technology, amongst other alternative treatments, to reduce the amount of dust particles which are

released during the surface roughening of adhesive bond primers on the airplane's fuselage onto which a paint primer and a topcoat are applied in the painting process.

In standard practice, the surface treatment of adhesive bond primers is: solvent cleaning with methyl ethyl ketone (MEK) followed by light abrasion with Scotch-Brite® (3M) and again cleaning with MEK to remove dust particles. This is a time consuming and unhealthy surface treatment process due to the formation of dust particles. Thus, a reference treatment and three physical surface treatments:

- Atmospheric plasma (10 – 120 seconds);
- Corona (10 – 40 seconds), or
- UV/Ozone (5 – 15 min.).

were done on bond primer protected chromic acid anodized aluminium test panels.

The test results were compared with the standard conventional three-step process: solvent cleaning, primer abrasion, and again solvent cleaning. After the surface treatment of the bond primer layer, a paint primer and paint top-coat were applied in a professional spray coating facility. The sequence of layers of the chromic acid anodized aluminium panels and those of the paint layers is shown in Figure 6.21. The test panels were coated with one of the following adhesive bond primers:

- BR® 127 corrosion inhibiting primer (Solvay);
- BR® 6700 NC a non-chromate water-based epoxy primer (Solvay);
- Redux 101 phenolic primer (Hexcel).

Figure 6.21 Schematic representation of chromic acid anodized aluminium with the adhesive primer and paint layers (not to scale).

The surface cleaning/activation effect on the three adhesive bond primers was studied by static water contact angle measurements. The test results (Figure 6.22) showed clearly the best overall wetting performance for UV/Ozone compared to atmospheric plasma and corona treatments.

After surface treatment of the three bond primers by UV/Ozone, atmospheric plasma, or corona, a paint primer (Akzo 37035 A), and a paint top-coat (Aerodur Finish C21/100) were applied. Subsequently cross-cut tests [99] and were done. The panels (Figures 6.23a and b) were cured according to the material specifications, and stored in the laboratory at room temperature for at least 1 week before cross-cut tests were carried out in laboratory conditions. The adhesion between the layers was evaluated in the initial dry state as well as after 14 days of tap water exposure at room temperature (RT). After removal from the water and drying of the panels further cross-cut tests were done (tape: Scotch 250, 3M, The Netherlands). Some of the visual test results on the test panels for the combinations of the adhesive primer with the paint primer and topcoat are presented in the upper sections of Figures 6.23a and b.

All three adhesive bond primers showed a rather similar behaviour as the prepared panels (either with paint primer or paint primer with topcoat) and showed no flaking during the initial (dry) state, as can be seen from the cross-cut test results. However, after exposure to tap water for 14 days at RT and subsequently drying, partial flaking, blister formation and detachment of the topcoat from the paint primer occurred, which

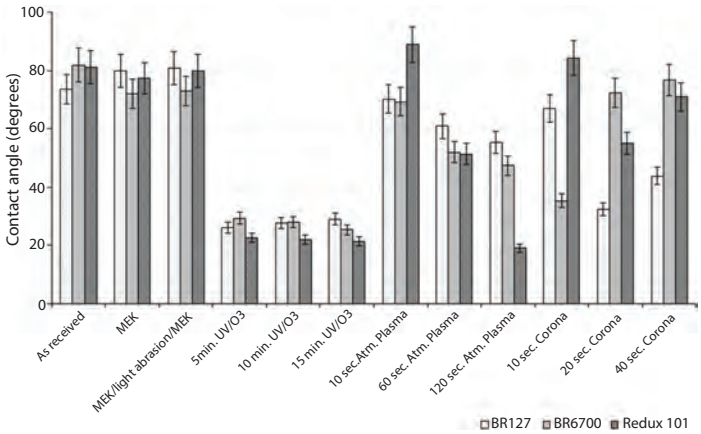

Figure 6.22 Static water contact angle data on three adhesive bond primers after various surface treatments.

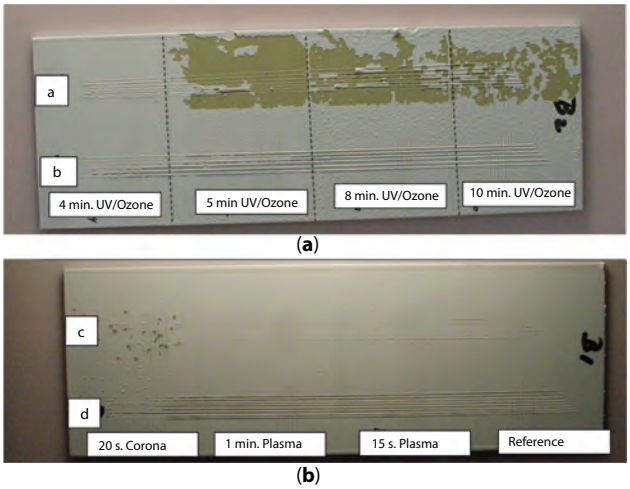

Figure 6.23 Cross-cut tape test results on chromic acid anodized BR127 primed together with paint primer and top coated panels after various surface treatments. The top section (a or c) of each panel is the 2 weeks water exposed part, and the lower section (b or d): non-exposed. The following surface treatments were done: a: 4, 5, 8 and 10 minutes UV/Ozone treated and painted, water exposed. b: 4, 5, 8 and 10 minutes UV/Ozone treated and painted, dry. c: 20 sec. corona, 60 sec. and 15 sec. plasma treated, the reference, water exposed. d: 20 sec. corona, 60 sec. and 15 sec. plasma treated, the reference, dry.

were obviously caused by a sub-optimal pre-treatment. This also occurred for the panels treated by UV/Ozone with treatment times longer than 4 min., possibly due to the generation of LMWOMs. The photographs of the test panels in Figure 6.23 show that the cross-cut test clearly differentiates between the quality of the dry and wet-exposed panels as well as the different surface treatment methods. These showed locally a rough topcoat surface due to blistering after the exposure and detachment of the topcoat and paint primer at these locations. All other panels showed flaking as a result of the scratch test, thus severe damage, especially with the total paint system (combined paint layer and topcoat). But no damage was observed for the reference panels and panels treated with plasma (15 sec. and 1 min.).

The above results show that either plasma (15 seconds) or UV/Ozone treatment (up to max. 4 min.) may be successfully used for the replacement of the conventional abrasion as a surface treatment for the adhesive primer layer before painting, thus excluding the generation of in the case of BR* 127, hexavalent chromium (Cr^{+6}), containing dust particles.

6.6.2.6 *Mechanical Tests on UV/Ozone Treated Epoxy Coated Magnets*

Static magnets of electro-motors were coated with an epoxy or a metallic coating to prevent corrosion. These surfaces were pretreated either by atmospheric plasma or UV/Ozone in order to improve the bonding to an adhesive. The physical surface treatments improved the surface wetting considerably compared to cleaning with a solvent wipe (methyl ethyl ketone, MEK) only, as can be seen in Figure 6.24.

Compared to the solvent wipe, a strongly increased surface wetting after UV/Ozone and atmospheric plasma treatments due to an increased surface polarity became visible, but no large difference in wetting between the two physical activation methods was evident. Generally, the best results were obtained either after 10 min. UV/Ozone or 60 sec. atmospheric plasma treatment. The resulting increase in polarity due to these physical surface treatments was expected to improve the adhesive bond strength between the coatings and a two-component room curing structural epoxy with 1 w% added glass beads of ø 150 µm or a no-mix acrylate adhesive. The adhesive bonds were pre-cured at room temperature for 1 day and then cured for 1 hour at 80 °C and 100 °C. Both shear (ASTM D1002 [100]) and butt joint tests (EN 15870 [101]) were performed on a 250 kN Zwick static test machine with a 1kN load cell. The lap shear and butt joint test results of the no-mix acrylate adhesive are shown in Figure 6.25. The lap shear test

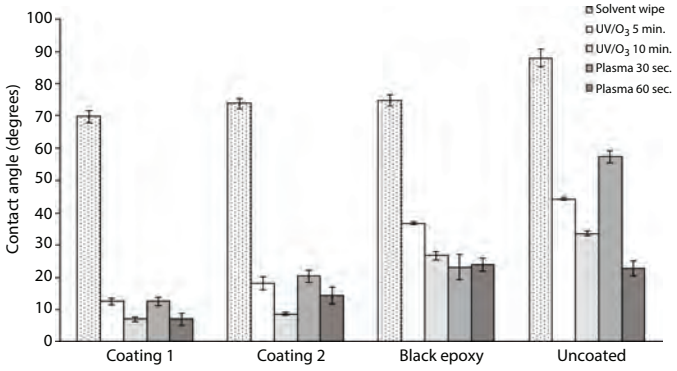

Figure 6.24 Static contact angles of water on magnet coatings after 5 different surface treatments.

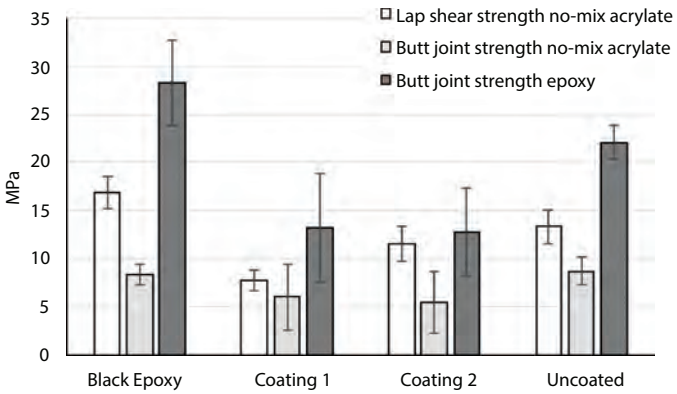

Figure 6.25 Lap shear strength together with butt joint test results for a no-mix acrylate and an epoxy adhesive on magnet coatings.

results of the epoxy adhesive bonds are not shown, but they were all at least twice as high as those found for the no-mix adhesive.

Fracture analysis of the lap shear and butt joint test samples for the no-mix adhesive showed that 90% of adhesion failure occurred on the coating surface. Magnets bonded by the epoxy adhesive showed 50% cohesive failure within the epoxy adhesive and 50% within the coating. The black colored epoxy showed about 90% cohesive failure of the coating itself, possibly due to too much filler material, increasing its brittleness.

The butt-joint test results were found to be the most discriminating for the failure type for both adhesives, with the black epoxy coating showing the largest pull-off strength. On average, the results of the no-mix acrylate adhesive showed a rather large scatter in results, most probably because the adhesive was not fully cured.

Generally speaking, when the more rigid epoxy adhesive was used, more cohesive failure in the coating occurred during mechanical testing.

6.6.2.7 UV/Ozone Modification of Poly(dimethylsiloxane)

Colloidal silver or gold was to be attached to the surface of a thin optically clear cast foil of a reticulated organosilicon compound Sylgard-184 poly(dimethylsiloxane) (PDMS), made from a two-component kit from Dow Corning. The viscoelastic PDMS, when cast as a foil, was to be placed on top of a valuable piece of art such as a drawing, photograph, or letter [e.g. 102, 103] for improved Raman analysis. The colloidal material functions to amplify the Raman signal and suppress the fluorescence of the

object. After analysis, the PDMS foil can easily be removed without leaving any traces.

The surface of the PDMS is highly hydrophobic and thus it has to be made more hydrophilic to allow adhesion of the colloidal particles. This can be done by exposing it to a so-called "piranha" solution, during which silicon oxide with hydrophilic (mainly –OH) groups are created on the treated surface [104]. However, this method was found to be too risky for the specific purpose (analysis of valuable pieces of art), non-uniform and also non-reproducible. A far simpler, safer and more reproducible method of surface oxidation was expected from exposure to an ozone generating low-pressure mercury lamp. In this process the macromolecules undergo chain scissions, involving both the main chain backbone and side groups, after which the UV-modified specimen interact with the molecular oxygen and ozone [105, 106]. The oxidised PDMS surface is then chemically reacted with (3-aminopropyl) triethoxysilane (APTES) and via this process amino groups are bonded to the PDMS which can then react with the colloidal material.

The "As received" cast PDMS surface (thickness ~ 1 mm) showed an average (water) contact angle of 98 degrees. But a surface treatment for 90 minutes by UV/Ozone resulted in a spectacular increase of the surface wetting with an average contact angle of 8 degrees (Figure 6.26). However, immediately after the treatment a "hydrophobic recovery" started and during such occurrence the chemical composition of the treated PDMS

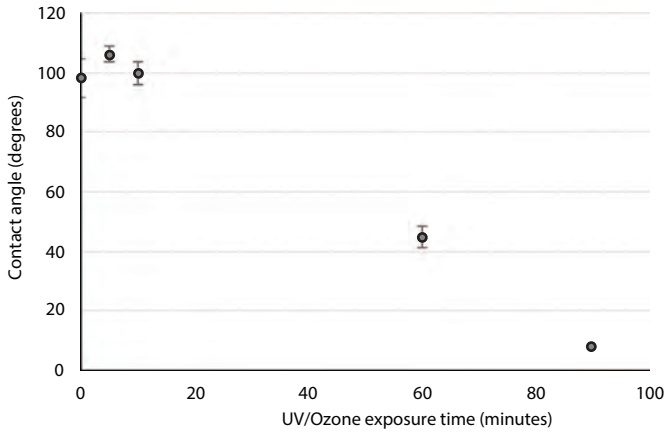

Figure 6.26 Static contact angle (water, degrees) on PDMS surface as a function of UV/Ozone exposure time.

surface changed over time due to the uncontrollable diffusion to the surface of non-crosslinked silicone oligomers through sub-microscopic surface cracks [105, 107, 108]. This cracking was not visible after the UV/Ozone treatment as shown by Owen and Smith [108]. Thus it is assumed that simply diffusion of hydrophobic molecules occurred. In contrast, the initial visible waviness of the surface as a result of casting was clearly visible in the micrograph (Figure 6.27a), but was removed by the UV/Ozone treatment. Indeed, after 60 and 90 minutes of UV/Ozone treatment (Figures 6.27b and 6.27c respectively) all visible signs of this waviness had disappeared.

Immediately after the UV/Ozone treatment the surface started to turn back to a hydrophobic state, which already became clearly visible within minutes and this increase of hydrophobicity continued (Figure 6.28). After 5 days exposure to a laboratory environment (20 °C, 55% RH) the same surface was exposed again to the UV/Ozone treatment for 90 minutes, after which it showed a complete wetting by water, though the trend to return to hydrophobic state started again directly after the treatment.

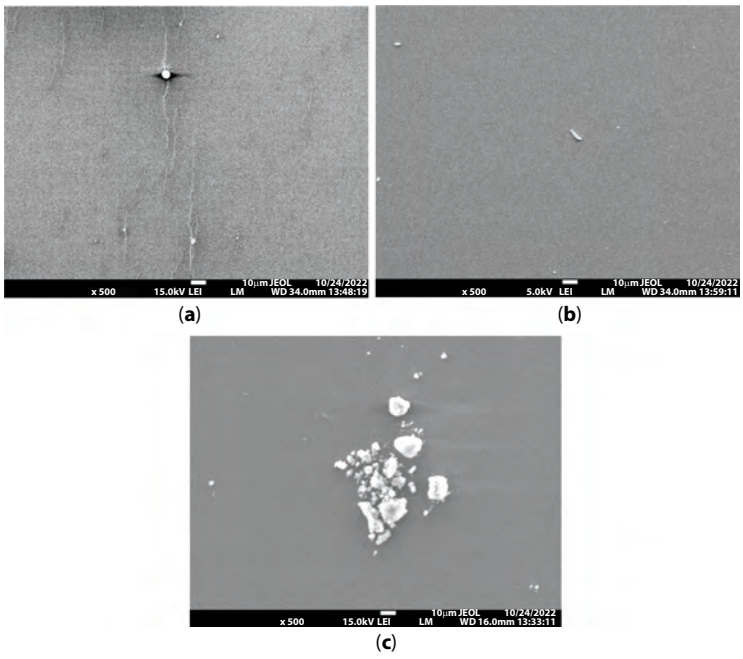

Figure 6.27 SEM micrographs of a cast PDMS surface after (a) 0 minute, (b) 60 minutes and (c) 90 minutes exposure to UV/Ozone.

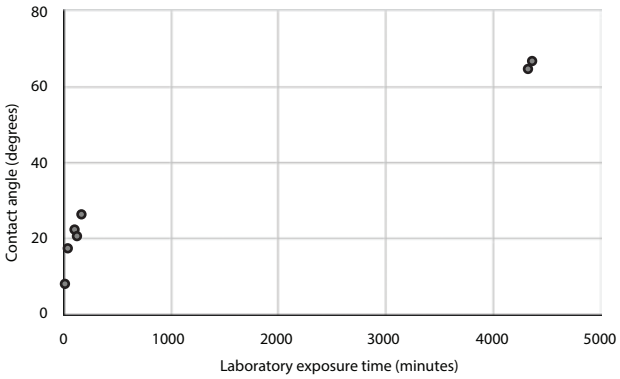

Figure 6.28 Static contact angle (water, degrees) as a function of the exposure of PDMS to laboratory air after an initial UV/Ozone treatment for 90 minutes.

6.6.3 UV/Ozone Treatment of Thermoplastics

6.6.3.1 Adhesive Bonding of POM to Aluminium

Small cylindrical stand-offs (ø 15 mm, thickness 5 mm) made of Polyoxymethylene (POM), an engineering thermoplastic, were bonded with a two-component paste adhesive to aluminium (2024 T3). These are used as cable guides in spacecraft constructions. However, the POM's surface free energy was found to be too low to obtain a reliable adhesive bond without adhesion failure on the POM surface to withstand at least 7 up to 33 temperature cycles between -100 °C and +100 °C.

Hence, different surface treatments were carried out to improve the bond strength. The POM surface was cleaned with isopropanol as a pre-cleaning step, roughened (emery paper P1000) and again cleaned with isopropanol (reference treatment, see Table 6.4). Then the samples were successfully treated for 5 to 20 seconds in 85% phosphoric acid at 50 °C, or exposed for 15 minutes to UV/Ozone, or exposed for 15 seconds to Corona. The adhesive bonding to aluminium was done either by the above-mentioned two-component room curing epoxy or a two-component silicone adhesive. After temperature cycles the bonded joints were tested in shear on a 20kN Zwick 1455 test machine with a 1kN load cell.

The average adhesive bond strength clearly improved by the UV/Ozone treatment (Figure 6.29), but the fracture areas still showed 100% adhesion failure at the POM surface. This failure is the result of a too large stress at the POM - adhesive interface during the temperature cycles as a result of the difference in thermal expansion between the POM and aluminium

Table 6.4 Surface free energy including the polar and dispersion components of POM after various surface treatments.

Type of treatment	Static contact angle (water, degrees)	Total surface free energy (mJ/m^2)	Dispersion component (mJ/m^2)	Polar component (mJ/m^2)
Reference (Degreased, roughened, degreased)	61	43	33	10
Degreased, roughened, degreased UV/Ozone (15 minutes)	38	58	24	34
Degreased, roughened, degreased, phosphoric acid	52	49	29	20
Degreased, roughened, degreased, corona (15 seconds)	42	56	28	28

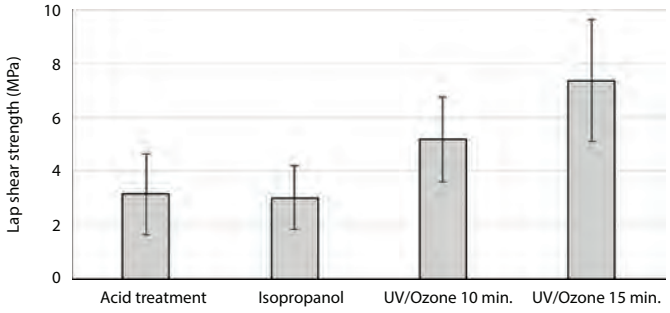

Figure 6.29 Average lap shear strength of POM bonded to aluminium with a 2- component room temp. curing epoxy (EC2216), as a function of surface treatment after 33 temperature cycles (from -100 °C to +100 °C).

substrate. Part of the solution was found by increasing the thickness of the adhesive bondline from 0.1 mm to 0.8 mm by adding 2 w% ø 0.8 mm glass beads to the mixed adhesive. An alternative solution might be to apply a more flexible adhesive and/or an increased density of polar groups on the POM surface.

6.6.3.2 Adhesive Bonding of Polyethylene (PE) to Stainless Steel

An instrument that was constructed from PE and stainless steel showed an adhesion bond failure at the surface of the PE. The part had to operate in a saturated saltwater environment at a temperature of -15 °C. The adhesive bond had to withstand this environment for up to 6 weeks. Therefore, it was decided to increase the hydrophilicity of the PE by a surface treatment.

Samples of both PE and stainless steel were pre-cleaned with ethanol before they were treated by UV/Ozone for 5 to 15 minutes which resulted in a strongly improved wetting performance for both materials (Table 6.5). Alternatively, the so-called DELO-SACO process was applied to the stainless steel [109].

After various surface treatments, the parts (PE to stainless steel) were bonded by a 2-component polyurethane adhesive with an adhesive bondline thickness of 0.2 mm, using 0.1w% glass beads. Samples were tested in shear (ASTM D1002) [100] and test results are shown in Figure 6.30.

Bond failure still occurred at the PE surface, despite the improved surface wetting as a result of any of the UV/Ozone treatments of the PE, and as a result, an increased bond strength, meaning that the combination of surface treatment and adhesive was not sufficient enough for this application. The data presented in Figure 6.30 show that the effect of surface treatment

Table 6.5 Contact angle of water on PE and stainless steel as a function of UV/Ozone treatment.

Type of treatment	Contact angle on PE (water, degrees)	Contact angle on steel (water, degrees)
No treatment	90	72
Ethanol	85	70
5 min. UV/Ozone	57	27
10 min. UV/Ozone	56	20
15 min. UV/Ozone	50	24

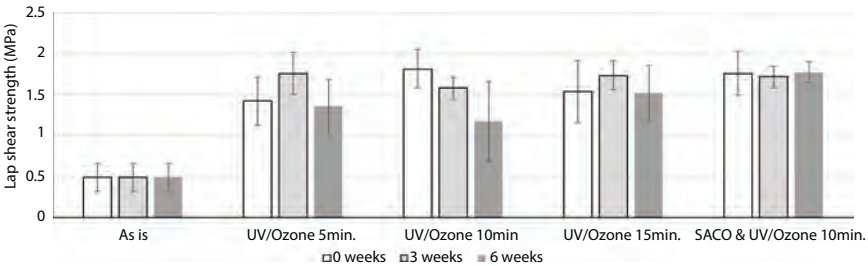

Figure 6.30 Lap shear strength test results of adhesively bonded PE to stainless steel after 0 to 6 weeks of aging in salt water at -15 °C as a function of various surface treatments.

by UV/Ozone leads to a strong increase in the adhesive bond strength, including after salt water exposure. Besides, the average bond strength after the DELO-SACO surface treatment with an added UV/Ozone treatment for 10 minutes showed a stable lap shear strength with time and an average bond strength in the same range as the UV/Ozone treatment alone, but with a slightly lower standard deviation.

It should be noted that the average bond strength reaches a maximum value, though not significant, at 10 min. of UV/Ozone treatment after which it reduces again due to the formation of Low Molecular Weight Oxidized Molecules (LMWOMs), further described in section 6.6.3.8.

6.6.3.3 Adhesive Bonding and Aging of HDPE

Only a few researchers have compared the effects of different physical surface treatments on surface wetting, adhesive bond strength, and relaxation of low energy surfaces [58, 110–112]. Hydrophobic materials with their non-polar nature such as polypropylene (PP), thermoplastic polyolefin (TPO) and High Density Polyethylene (HDPE) are generally difficult to bond adhesively, and therefore need some kind of surface treatment prior to the adhesive bonding process [109]. Sometimes a specific primer (a chlorinated polyolefin in an organic solvent) is used to increase the surface polarity for an improved interaction with the adhesive [113–115].

The physical surface treatment of high density polyethylene (HDPE) used as a construction element of a fuel container was investigated. The treatment had to provide an increased surface wetting to improve the lap shear strength performance after adhesive bonding. The HDPE material was pre-treated with a commercial cleaning solvent mixture called PFQD [116] as a pre-cleaning, after which any of the following physical surface treatments was used:

- UV/Ozone treatment: using three 80 W Heraeus Noble Light (NNIQ120) low pressure UV-lamps at a distance of 20 mm from the surface and a treatment time between 5 and 30 minutes;
- Corona treatment: at a distance of 10 mm from the surface and treatment times between 15 and 75 seconds;
- Atmospheric plasma treatment: at a distance of 10 mm from the torch and treatment times between 5 and 20 seconds.

The resulting effects of these treatments on the wetting by water of the HDPE surface as a function of the treatment time can be found in Figure 6.31.

The adhesive bonding was done using a mechanically relatively weak methyl methacrylate (MMA) adhesive specifically suited for bonding thermoplastic adherends, although acrylic adhesive types exist that might give a much higher strength (up to 7 MPa).

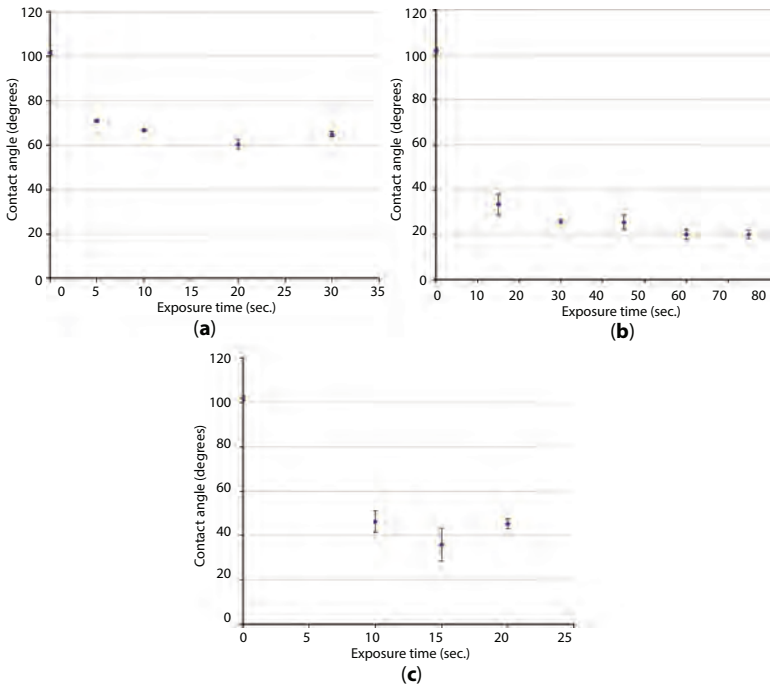

Figure 6.31 Static contact angle of water on HDPE as a function of the surface treatment time by UV/Ozone, corona or atmospheric plasma treatment. Please note the different time scales on the horizontal axis. (a) UV/Ozone. (b) Corona. (c) Atm. Plasma.

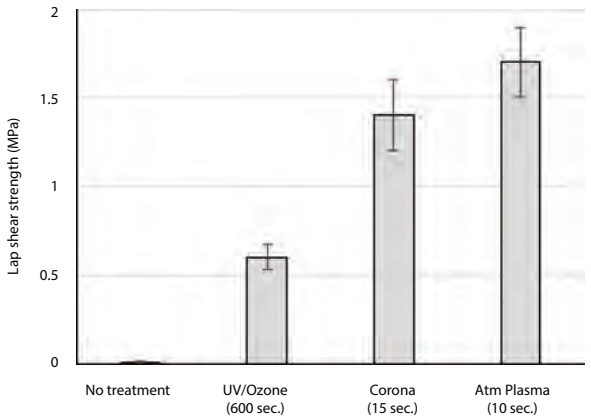

Figure 6.32 Lap shear strength of HDPE bonded to HDPE by a two-component epoxy as a function of various surface treatments.

Destructive mechanical lap shear tests were performed by ASTM D1002 [100] on a 250 kN Zwick tensile test machine with a 1kN load cell at a speed of 0.13 mm/min. Test results (Figure 6.32) show that atmospheric plasma and corona treatments are more effective than UV/Ozone and result in a large increase of bond strength compared to the untreated surface, which showed hardly any bond strength. This is in agreement with the results of the static water contact angles (Figures 6.31a-c), where the wetting as a result of the UV/Ozone treatment was also less than that by the other two physical surface treatments (corona and atm. plasma).

6.6.3.4 Adhesive Bonding of Polyethylene (PE) to Acrylonitrile Styrene Acrylate (ASA)

PE was bonded to acrylonitrile styrene acrylate (ASA) by a modified silane (MS) Polymer adhesive as a part of a pipe construction for use at elevated temperatures. However, initially the adhesive bond strength (with a silicone hot-melt adhesive) was found to be less than 0.2 MPa at 65 °C, showing 100% adhesion failure at the PE surface, which was insufficient.

ASA is an amorphous thermoplastic material, which is often used in the automotive industry as an alternative to acrylonitrile butadiene styrene (ABS) as it has a far better weathering resistance, especially to UV light. PE is one of the most often used common plastics today with many applications in packaging (bags, films, containers), but it is also a non-polar material, showing poor wetting characteristic and a low surface free energy

(~30 mJ/m^2) and is thus difficult to bond without (physical or chemical) treatment or the use of specific polyolefin primers [117, 118].

Various surface treatments were investigated in order to increase the initial bond strength as well as the durability of the adhesive bond. Thus, the following surface treatments were chosen:

- Solvent cleaning, roughening (Scotch-Brite®);
- Making use of a coupling agent/primer;
- Activation by UV/Ozone or atm. plasma.

An MS polymer was chosen as an alternative to the original hot-melt adhesive, which provided the opportunity to make use of a dedicated polyolefin primer system on the PE (Figure 6.33).

The optimum average lap shear strength was found by testing the adhesive bond in shear (ASTM D1002). Just roughening the surface did not lead to any improvement in the bond strength, as it still lacked polarity for adequate adhesive bonding. Nor the use of atmospheric plasma or a primer showed convincing improvement in the max. shear strength of the bonded samples. However, the surface treatment that led to a highly improved adhesive bond strength and 100% cohesive failure within the adhesive was found to be a 5 to 10 minutes UV/Ozone treatment (Figure 6.33).

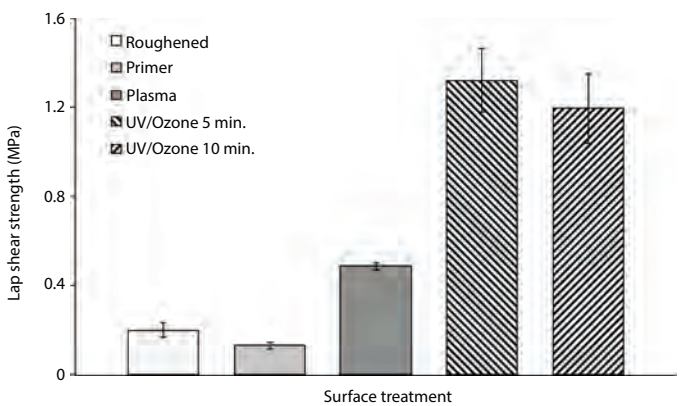

Figure 6.33 Comparison of different types of surface treatment methods on the lap shear strength of PE bonded to PE by an MS polymer adhesive.

6.6.3.5 Adhesive Bonding of Polypropylene (PP)

The surface functionalisation by photo-oxidation and the resulting increase of the adhesive bond strength to hydrophobic materials such as pure PP and PE was investigated by adhesive bonding with a one-component MS polymer mixed with 1 w% glass beads with a diameter of 0.125 mm. Bonded samples were cured for at least a week at RT. The test results from the lap shear strength measurements (ASTM D1002 [100]) are shown in Figures 6.34a and b, respectively.

All samples failed 100% at the interface when untreated. The fracture surfaces of the PP lap shear joints treated by Excimer 172 nm moved gradually from 100% interfacial failure without surface treatment to 100% cohesive failure within the adhesive layer after 15 seconds of photo-oxidation. After the surface treatment either by the Excimer 222 nm or the low-pressure mercury lamp, the failure mode changed to 100% cohesive failure in the adhesive layer. But the highest bond strength with both materials was obtained when the low-pressure mercury lamp was used. For the surface treatment of PP, the 222 nm Excimer is clearly more effective than the 172 nm. Though for PE the 172 nm seems to give better results, which are reached after an exposure time of only a few seconds.

6.6.3.6 Surface Treatment of Nylon (Polyamide 6)

Polyamide 6 (nylon) is an important structural material used in numerous industrial sectors. Surface treatment prior to adhesive bonding had been successfully demonstrated before using various methods like ozone gas only [119], plasma [120], or corona [121] treatments, but not yet by UV/Ozone treatment.

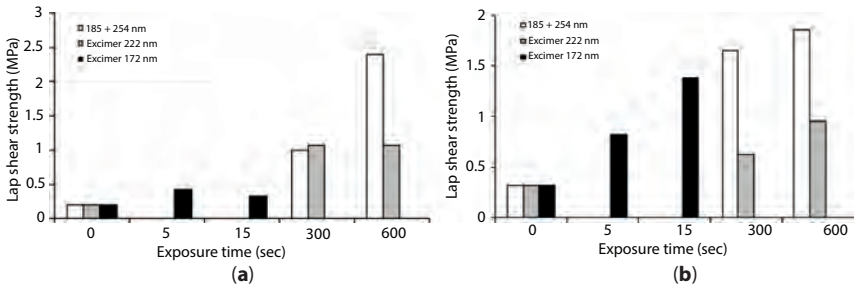

Figure 6.34 Lap shear strength as a result of the exposure time of PP (a) and PE (b) to: a low-pressure mercury UV-source, an Excimer 222 nm and an Excimer 172 nm. The bonded samples were made of PP to PP and PE to PE joints.

A flexible hollow nylon cylindrical tube was found to have occasionally adhesion bond failure when bonded to a stiff cylindrical housing of polycarbonate by an urethane/methacrylate UV-curing adhesive blend. Nylon is known for its absorption of water, which is, in practice, frequently found to be the reason for a premature adhesion failure in bonded structures. However, pre-drying the parts was found to be impossible at the production site. For this reason only a small set of samples was pre-dried in a stove in the Adhesion Institute of the Delft University of Technology laboratory for 2 hours at 60 °C in order to investigate the sensitivity of the chosen adhesive to absorbed moisture. The mechanical data did not show any improvement in the adhesive bond strength nor in the failure type, and pre-drying was therefore not included in the adhesive bonding process.

All parts were physically pre-treated either by UV/Ozone or corona in order to obtain the largest possible number of polar groups on the surface to obtain more molecular interactions between the nylon surface and adhesive.

Initially, the dispersion component contributed about three times as much to the surface free energy than the polar component (Figure 6.35). This contribution decreased as a function of the treatment time as a result of decreasing material density. In contrast, the value of the polar contribution more than doubled after either of the two physical surface treatments. After 5 seconds corona treatment the nylon parts show an increase in the polar component together with an increase in the total surface free energy. The contribution of the average polar component to the surface free energy is even larger than the one obtained for the UV/Ozone treated samples, though not significant.

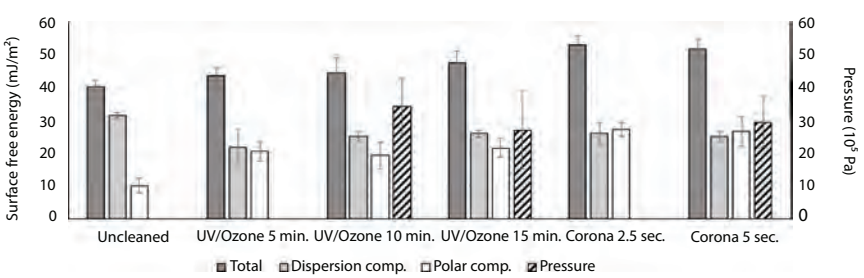

Figure 6.35 Bar graphs representing the surface free energy of nylon including its dispersion and polar components. The diagonally hatched bar graphs show the mechanical test results (due to an applied liquid pressure) after adhesive bonding to a polycarbonate housing.

10 and 15 minutes of UV/Ozone and 5 seconds of corona were used as surface treatments before testing the adhesive bond strength. The mechanical strength was tested by applying a hydrostatic pressure of 1 bar/second to the nylon tube which resulted in a peel force on the adhesive bond. The average adhesive bond strength (measured as a pressure until failure) was found to result into the highest value after 10 - 15 minutes of UV/Ozone treatment (Figure 6.35). But, within the standard deviation, no difference is visible between the results. Although the adhesive bond strength increased, the failure type remained 100% adhesion failure at the nylon surface as a result of the highest stress peaks which naturally occur near the surface of the most flexible adherend of the adhesive bond.

6.6.3.7 UV/Ozone Treatment of Poly(phenylene sulphide) (PPS)

Some parts of the Airbus A340-600 aircraft are made from (PPS), a thermoplastic matrix reinforced with either carbon or glass fibres. The parts made of these hybrid materials are difficult to bond adhesively, due to the high chemical resistance of PPS and its low surface free energy. Some research has been published regarding its adhesion behaviour after low pressure plasma treatment [122]. Hence, an alternative physical surface treatment such as UV/Ozone was investigated in order to increase the surface free energy. Therefore, 20 samples were selected for further testing:

- 8 samples were made of PPS/carbon fibre (2 were roughened by sandpaper);
- 8 samples were made from PPS/carbon fibre/Astrostrike® (an aerospace lightning strike damage and shielding protection material) which included a nonwoven copper mesh, two of which were roughened with sandpaper;
- 4 samples were made of PPS/glass fibres.

Static contact angle measurements using diodomethane, tricresyl phosphate, formamide, glycerol and double distilled water showed that the surface treatment increased the wetting of water as a result of the increased polar component of the surface free energy of the matrix material, which increased from 10 (Figure 6.36a) to over 40 mJ/m^2 (Figure 6.36b). This last value was obtained after 5 minutes of UV/Ozone treatment, independent of the filler material (Figure 6.37). No further increase of the polar component could be found after about 5 minutes UV/Ozone exposure.

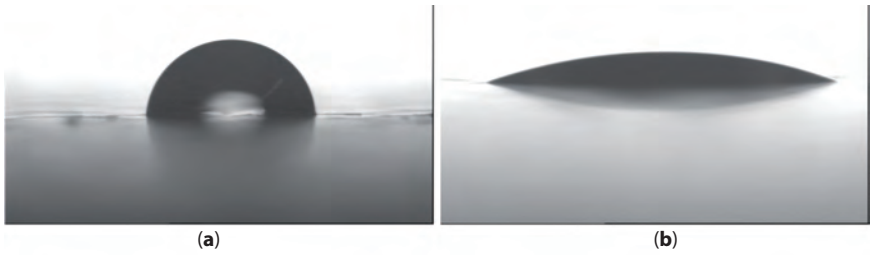

Figure 6.36 Double distilled water droplets (volume 3 microliters) on PPS, (a) without treatment, and (b) after 5 minutes of UV/Ozone treatment.

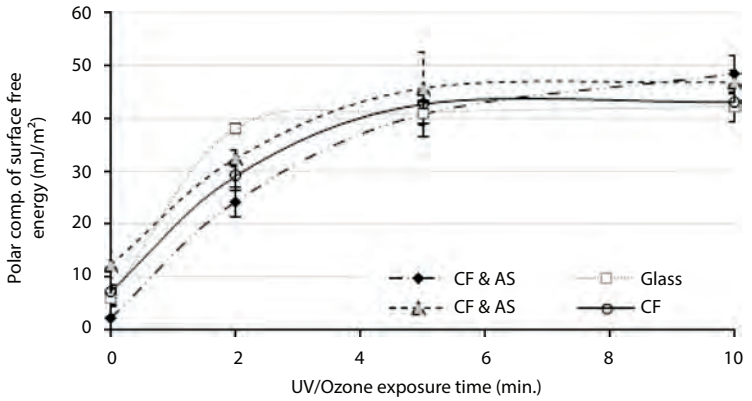

Figure 6.37 Trend lines connecting the measurements of polar component of the surface free energy of PPS as a function of the UV/Ozone treatment time. Abbreviations of filler materials: CF: Carbon fibres, AS: Astrostrike® lightning protection.

The gain in the polar component of the surface free energy had the implication that adhesive bonding by a two-part structural paste adhesive curing at RT became now successful. No significant difference could be found in the surface free energy in relation to the used filler materials. However, the dispersion component of the surface free energy slightly lowered during the surface treatment due to the effect of reduced polymer density, which compensated for the polar increase.

6.6.3.8 UV/Ozone Treatment of Poly(methyl methacrylate) (PMMA)

Generally, physically treated polymer surfaces show a maximum in the wetting performance as a function of treatment time. However, just slightly before this maximum wetting value is obtained, a reduction of the adhesive

bond strength is often measurable. This is the result of the creation of small sized functional polymer groups on the outer surface, called Low Molecular Weight Oxidized Molecules (LMWOMs), which are mechanically less strongly connected to the inner mass [6, 45].

Examples of this phenomenon, and thus in agreement with what other researchers have found, can be seen in Figure 6.38, which shows the PMMA surface free energy and its components, on the left-hand vertical axis, together with the mechanical lap shear test results, on the right hand side vertical axis, as a function of three different UV/Ozone exposures: 0, 5 and 10 minutes in a single graph. The average polar component is shown to increase up to an exposure time of 10 minutes. The failure type changed from 100% adhesion failure on the non-treated PMMA surface to 100% cohesive failure within the silicone adhesive after 5 minutes of surface treatment. This was in line with the increase of the polar component. However, further study of the lap shear strength and failure type clearly showed that an exposure time of more than 5 minutes resulted in a slight average decrease of bond strength (though not significant) together with an increase of the polar component. This is a general observation that can be made with the physical surface treatments: The density of polar groups, including low molecular weight oxidized material (LMWOM), is still increasing which coincides with the start of a decreasing adhesive bond strength as a function of treatment time. This is the effect of the deterioration of the surface layer due to polymer chain scissions by the

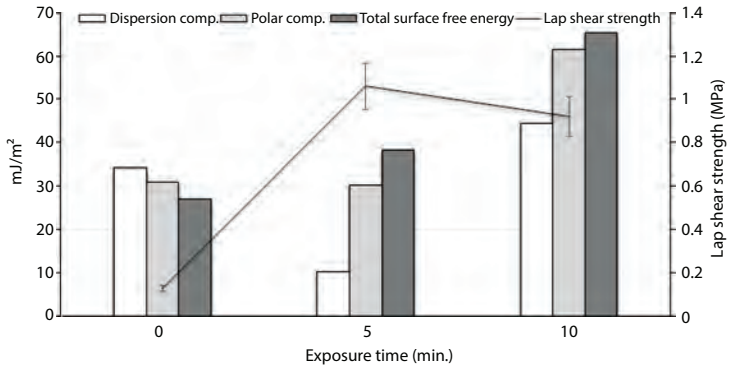

Figure 6.38 Total surface free energy (mJ/m^2) of PMMA, including the dispersion and polar components (left hand side vertical axis) shown as a function of the UV/Ozone treatment time. The lap shear strength of PMMA bonded to PMMA by a silicone adhesive is shown on the vertical axis (MPa) on right-hand side of the graph.

UV-light and oxidation, resulting in the formation of LMWOM which are less strong attached to the bulk mass, eventually weakening the adhesive bond strength.

6.6.3.9 Adhesive Bonding of Flexible Polymeric Solar Cells

A key issue in the development of solar powered vehicles is the adhesive bonding and framing of solar cells by an adhesive tape with gap filling ability and the capability to deform. The flexible solar cells were encapsulated in fluorine-based plastic foils, poly (ethene-co-tetrafluoroethene) (ETFE, Tefzel®), with a surface free energy ~30 mJ/m^2 or poly (ethene-co-chlorotrifluoroethene) (ECTFE, Halar®) as an alternative (semi-crystalline) encapsulating material, which shows high corrosion resistance and strength in a wide temperature range.

A large number of surface treatments are available, though practically rather limited for the above materials and application, as fluoropolymers are resistant to most oxidizing agents and solvents and solar cells are too sensitive to be treated by corona or flame treatments. Still, the resulting surface topography and chemistry should be optimised to the characteristics that best fit to those of the chosen adhesive. For this reason, several passive chemical cleaning agents and physical and mechanical treatments of the encapsulating foils were compared before being bonded, as a decisive factor in the successful bonding of low surface free energy substrates. Any such treatment should always start with degreasing the substrate using a cleaning agent. The preferred cleaning agents for fluorocarbons are chlorinated alcohols or ketone solvents. The solvent can be applied by wiping the surface in one direction using a special paper or a clean cloth. But the highest efficiency of degreasing can be obtained by ultrasonic agitation of the substrate submerged in a detergent solution.

In this case, alternative physical treatments were investigated, and for this reason all specimens were degreased with a commercial solvent mixture called PFQD [116] using a paper or cloth before the physical treatment took place. Only abraded specimens (D-Ab) were degreased again in order to remove dust particles.

Figure 6.39 displays the average static contact angle of double distilled water including the standard deviation indicating that ECTFE showed an overall better wetting (lower contact angle) than ETFE. This is due to the chloride group in the molecule's backbone giving rise to a higher surface polarity. The standard deviation is high for DP-60 and D-Ab-P60 both

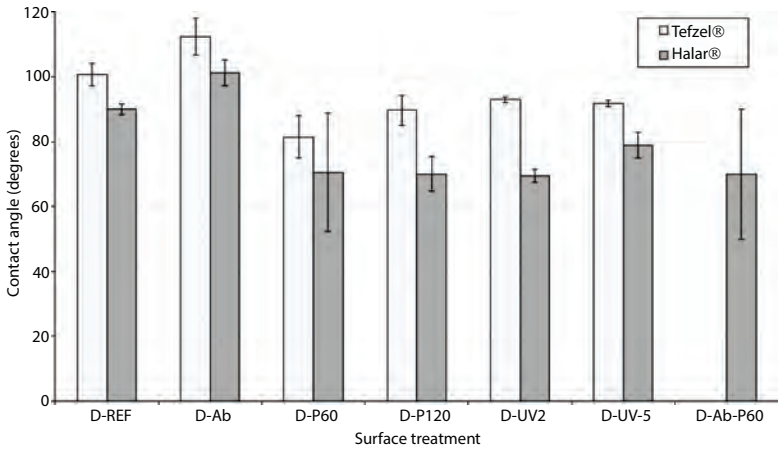

Figure 6.39 Static contact angle measurements (double distilled water) on poly(ethene-co-tetrafluoroethene) (ETFE, Tefzel®) and poly(ethene-co-chlorotrifluoroethene) (ECTFE, Halar®) surfaces as a function of the surface treatment. D-: degreased by solvent only, Ab: abrasion, P60, P120: respectively 60 and 120 seconds atmospheric plasma, UV2, UV5: respectively 2 and 5 minutes UV/Ozone treatment, Ab-P60: abrasion followed by 60 seconds atmospheric plasma treatment.

involving 60 seconds of open air plasma treatment, as can be found in the bar graph. The reason for this phenomenon is the difference of the direction of the focussed plasma beam torches angles (-45°, 0°, -45°) relative to the surface. Furthermore, it can be concluded that:

- Halar® showed a better average wetting performance (lower contact angle with water) than Tefzel®. This difference resides in the chlorine atoms in ECTFE, which are substituted by a fluorine atom in the structure of ETFE;
- There was no noticeable wetting difference between 60 sec. plasma and 120 sec. plasma treatments. However, some de-colourisation of the surface occurred when exposed to a 120 sec. plasma treatment;
- There was a large deviation in the test results of the 60 sec. plasma treatments, due to the sensitivity to the nozzle angle used;
- The lowest, and most consistent, contact angle was established on Halar® foil by degreasing, abrading and 60 sec. plasma treatment. The resulting contact angle was 54°;

- Worst wetting, or highest contact angle, was obtained after abrading the Tefzel® foil, as abrading only improves the wetting for surfaces with a contact angle below 90°;
- UV/Ozone treatment led to a good wetting performance, and resulted in contact angles roughly comparable to atmospheric plasma;
- The UV/Ozone treatment results showed a slightly lower standard deviation than the ones obtained with atmospheric plasma surface treatments and/or abrasion.

6.6.3.10 Treatment of ABS for Adhesive Bonding

Acrylonitrile butadiene styrene (ABS) is a lightweight, hard and impact resistant low-cost amorphous polymer. As a result, it is often used as a housing material for consumer products, especially in the automotive industry. However, some kind of surface treatment is often needed to obtain a reliable adhesive bond [123].

A poor peel adhesion with an adhesion failure of 100% was found when ABS parts were bonded with a polyurethane adhesive without surface treatment, except degreasing. For this reason mechanical and two physical (atmospheric plasma and UV/Ozone) surface treatments were investigated in combination with different types of adhesives.

After pre-cleaning with PFQD, a commercial degreaser [116], the mechanical abrasion was done using grade 500 emery paper which visually showed a clear increase of the surface roughness. This step was followed by cleaning (again) with PFQD to remove the generated dust particles.

During the second set of experiments the physical surface treatments were done. After solvent cleaning with PFQD to remove most of the organic contaminations, either atmospheric plasma or UV/Ozone surface treatments were carried out in order to improve the wetting performance.

Static contact angle measurements using water were done to determine the best wetting performance. Plasma treatment was found to improve the surface wettability but to a lesser extent than the 4 minutes of UV/Ozone treatment (Figure 6.40). Hence, a PFQD [116] pre-cleaning together with 4 min. UV/Ozone treatment showed the best wetting results with an average contact angle of 28 degrees.

After a sequence of surface treatments, which always started with a pre-cleaning with PFQD (Figure 6.40), the substrates were bonded with four different adhesives (2 different types of methacrylate and two different one-component polyurethanes).

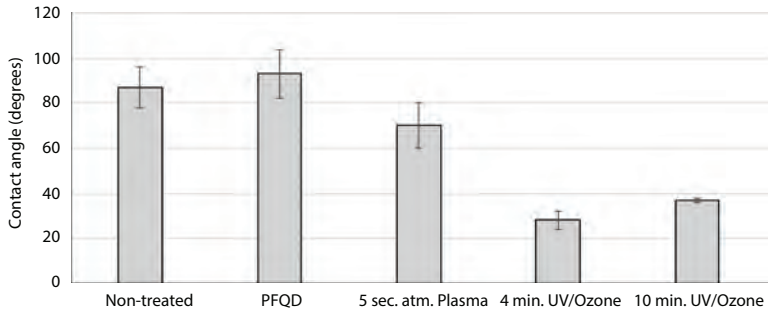

Figure 6.40 Static contact angle of water on an ABS surface "as is" and after solvent pre-cleaning with PFQD followed by atmospheric plasma or UV/Ozone surface treatments.

After the adhesives were fully cured at RT mechanical tests were done according to ASTM D D1876 [124] on a 20kN Zwick test machine using a 1kN load cell (Figure 6.41).

All alternative treatments showed an increase in the peel strength, compared to the original test results (non-treated or "as is"), especially when abrasively treated (Figure 6.42). In the "As is" & PU (1) the failure mode was found to be 30% – 70% interfacial on the ABS surface, while adding abrasion changed the failure mode to 90% cohesive failure within the adhesive layer.

The use of the methacrylate adhesive changed the failure mode to a cohesive failure within the ABS material, meaning that the ABS was weaker than the adhesive bond, and at the cost of an increasing standard deviation when UV-light is used in combination with mechanical abrasion.

The main results of this research, which show an increased adhesive performance when abraded and/or physically treated by e.g. atmospheric plasma treatment, are in agreement with those found by Frascio *et al.* [123].

Figure 6.41 Typical example of a peel test on one of the ABS samples tested according to ASTM D1867.

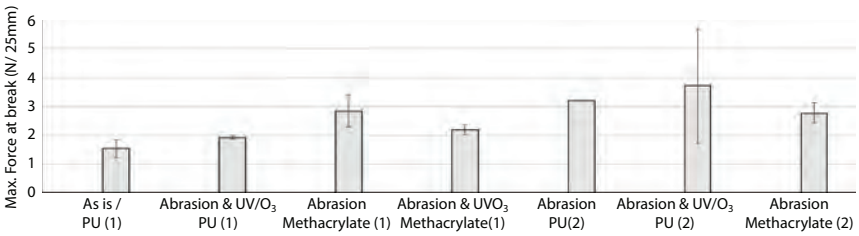

Figure 6.42 Maximum peel force at break for ABS bonded to ABS as a function of various surface treatments and adhesives. Peel strength by ASTM D1867. Not shown on the x-axis is the effect of only cleaning with PFQD, carried out prior to the presented surface treatments.

6.6.3.11 Adhesive Bonding of Styrene-Acrylonitrile (SAN) to a Thermoplastic Elastomer (TPE)

UV/Ozone treatment was used as one of the physical surface treatments to improve the adhesive bond strength of a silicone sealant to an injection moulded medical product that consisted of a glass-filled styrene-acrylonitrile (SAN) resin, a colourless and transparent thermoplastic, bonded to either a thermoplastic elastomer TPE (an unknown mixture of a plastic and a rubber) or to synthetic quartz glass.

Various surface treatments were carried out on the SAN, TPE and the quartz glass surfaces in order to improve their wettability and to obtain a higher initial bond strength. The adhesive bonding was done with a light-curing epoxy adhesive.

Figure 6.43 shows the results of the static contact angle measurements with water. A large standard deviation with unknown origin is observed in the obtained data which shows that neither degreasing nor plasma or corona treatment were able to increase the wetting performance of SAN material. However, the 10 min. UV/Ozone treatment did decrease the average contact angle (with water) and showed the best wetting results.

In contrast to the results found for SAN, treating TPE by UV/Ozone hardly influenced the contact angle, most possibly because the reduction in the density of the polymer is larger than the increase in the polar component, as it seemed that hardly any oxidation of the TPE surface had occurred.

The observed effect of the 5 min. UV/Ozone surface treatment on quartz led to spontaneous surface wetting, indicating a (near to) zero contact angle, a result which was often observed on glass and quartz materials by the authors.

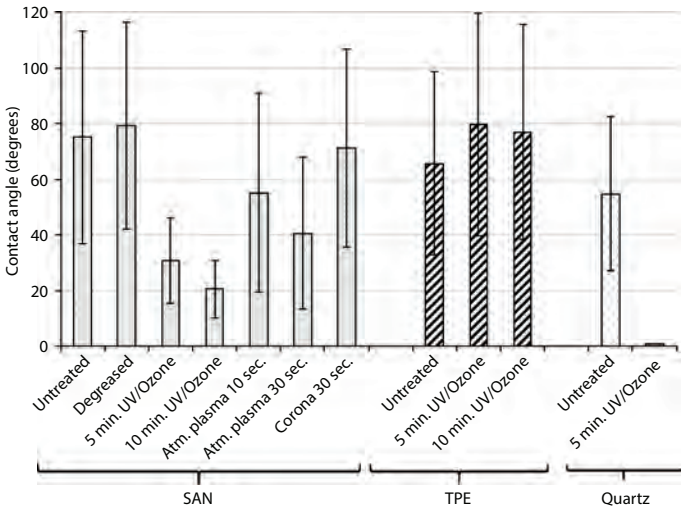

Figure 6.43 Test results of the static contact angle measurements (water) on SAN, TPE and Quartz after various surface treatments.

6.6.4 UV/Ozone Treatment of Rubbers

6.6.4.1 UV/Ozone Treatment of SBS Rubber

SBS rubber is a block copolymer and a special type of rubber that can be classified as a thermoplastic elastomer; it behaves like a rubbery material at room temperature without being crosslinked like most other rubbers, though at higher temperatures it can be moulded into a specific shape. This characteristic makes it useful for applications like tire treads and the soles of shoes where material durability is an important aspect. However, the material is non-polar, and as such difficult to bond without a specific surface treatment. As chemical treatments generate large amounts of hazardous waste, or require expensive instrumentation [e.g 125] UV/Ozone treatments were investigated as an alternative [47].

As regards the Excimer 222 nm, a small but steady increase of polar group density on the surface as a function of treatment time up to 15 minutes was formed after which the static contact angle with water became almost zero (Figure 6.44a). But the effect flattens out when the maximum density of polar groups is reached as the density of the non-polar component is steadily decreasing as a function of exposure time due to a decrease of the molecular density.

The low pressure mercury lamp showed a steady increase of both the polar and dispersion components. Though the molecular density started to decrease after about 5 minutes of exposure (Figure 6.44b).

After 15 minutes, both surface treatments resulted in an increase of the total surface free energy as a function of treatment time which was up to three times as high as the initial value.

The highest average lap shear strength of the SBS rubber was obtained by the longest exposure time to both the Excimer 222 nm and the low pressure mercury lamp (Figure 6.45). It is thus worth mentioning that for SBS-rubber the effect of the Excimer 222 nm on the adhesive bond strength is roughly the same as that of the low pressure UV-s ource. The adhesive bond strength is strongly increased after a surface treatment with either UV/Ozone equipment. The type of bond failure after both UV/Ozone treatments, independent of the treatment time, moved from 100% adhesion failure at the interface to about 50% cohesive failure in the adhesive layer. These results are in agreement with the results found by Romero-Sánchez *et al.*, who studied the influence of different loadings of fillers in relation to the UV/Ozone treatment time and the adhesion to polyurethane adhesive [7].

6.6.4.2 *Surface Treatment of Ethylene Propylene Diene Monomer (EPDM) Rubber to Optimize the Adhesion of a Coating*

EPDM is an elastomer, resilient up to 600% elongation, extremely durable and for these reasons finds its use in commercial products such as roof covers (housing) and as (coated) door seals in automotive and refrigerator constructions. The investigated EPDM rubber had to be coated for cosmetic reasons for the application as an automotive car door seal.

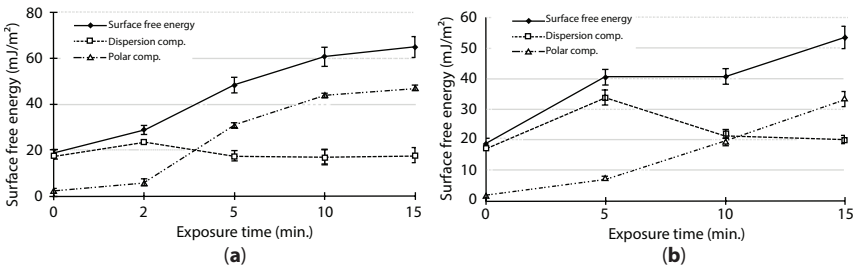

Figure 6.44 Surface free energy of SBS-rubber as a function of treatment time by (a) a 222 nm Excimer and (b) a low-pressure mercury lamp.

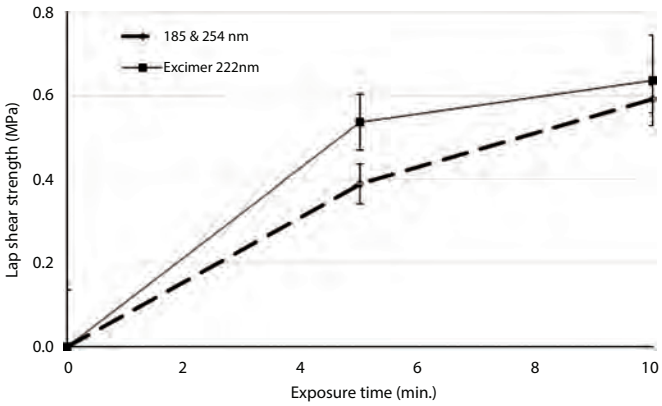

Figure 6.45 Bond strength of SBS rubber bonded to SBS rubber after the surface treatment by an Excimer 222 nm or a low pressure mercury light source.

Therefore, an alternative surface treatment was investigated for the generally applied labour-intensive and unhealthy solvent–based cleaning procedure. Various surface modification methods for EPDM have been published in literature, most of them are based on plasma treatments either with [126], or without [127–129] organosilicon precursors, but also UV/Ozone surface activation as an adhesion promoting treatment was described by Hamdi and Poulis [130].

6.6.4.3 EPDM Rubber Pre-Treated by a Low Pressure UV-Source

An industrially often used sequence of surface preparation steps before applying a coating on rubber materials is:

1. Removal of dust from the rubber samples and degreasing by means of wiping with a piece of cloth soaked in a solvent in one direction;
2. Storing the cleaned samples in a rack, often for several hours to a day;
3. Applying a primer to the samples (manual-spraying);
4. Drying of the primer;
5. Application of the final coating (manual spraying);
6. Drying of the coating in an oven.

UV/Ozone treatment was investigated in order to reduce the number of production steps and thus a simplified production that was less labour

intensive. Therefore, contact angle measurements, using different liquids, were done on an EPDM-rubber surface after treatment by a low-pressure mercury UV-source in order to determine its effect on the surface free energy. The results are presented in Table 6.6.

These measurements clearly reveal an increase of polar surface groups and a decrease of the dispersion component as a function of treatment time by the low pressure UV-source. The effect on the adhesion of the coatings applied to the UV/Ozone treated and untreated samples is shown in Table 6.7. Note that a pre-cleaning step by means of a solvent (naphtha) was done to the non-UV/Ozone treated samples. After UV/Ozone treatment for 0, 5 and 10 minutes a solvent-based primer was applied to 50% of the samples after which an electrostatic paint coating was applied.

The adhesion of the paint coating was tested by measuring the pull-off force of the coating from the substrate by the cross-cut test (ISO 2409 [99]). Six parallel scratches were made in two perpendicular directions by means of a certified tool consisting of a set of sharp knives. Subsequently a tape was applied and pulled off within 5 minutes. The more the squared coating patches remained on the surface, the better the level of adhesion.

The final coating was thus applied to both primed and un-primed samples. The untreated samples showed no adhesion whatsoever to either the primer or combination of primer and/or coating due to too low surface free energy as a result of lack of EPDM polar surface groups. The naphtha-only cleaned samples were used as a reference which showed a better performance but still showed unsatisfactory adhesion test results. Test results of all UV/Ozone treated EPDM samples showed a strongly

Table 6.6 Surface free energy of EPDM-rubber as a function of surface treatment time using a low pressure UV-source. Please note that the measured value of the solvent (naphtha) cleaned rubber is only temporary due to adsorbed solvent.

Type of treatment	Total surface free energy (mJ/m^2)	Dipersion component (mJ/m^2)	Polar component (mJ/m^2)
Not treated	29.7	24.9	4.8
Solvent treated	46.4	24.5	21.9
5 minutes UV/ Ozone	44.7	22.5	22.2
10 minutes UV/ Ozone	46.7	20.7	26.0

Table 6.7 Surface free energy and coating adhesion to the EPDM-rubber as a function of surface treatment by a low pressure UV-source. Each presented result is the averaged value of 4 different samples.

Type of treatment	Total surface free energy (mJ/m^2)	Adhesion of coating with primer	Adhesion of coating without primer
Not treated	29.7	n.a.	n.a.
Solvent cleaned	44	50%	n.a.
5 minutes UV/ Ozone	44.7	good	good
10 minutes UV/ Ozone	46.7	good	good

improved adhesion performance: the coating showed no more adhesion failure during the tape test [99]. Thus it can be concluded that the UV/ Ozone treatment not only gave satisfactory results from the point of view of the quality aspect, but also offered the opportunity to reduce the number of production steps.

6.7 Prospects

Ongoing investigations lead to new technological developments in physical surface treatments for plastics. This is stimulated by the increasing use of water-based printing inks, adhesives and coatings which require polymer surfaces to be treated to increase their surface free energy. Different methods such as chemical, mechanical or physical treatments like UV/ Ozone, corona, flame, atm. plasma, etc. might improve their wetting property resulting in a higher initial adhesion strength and long-term stability in structural applications [131, 132]. However, the developments and commercial applications of equipment that produces UV-C light and ozone gas for surface cleaning and specific functionalisation are still far behind the many available "alternatives".

This is a pity, as despite its successful treatment results, low investment costs, ease of use, surface cleaning capability (both for polymers and metals), up to the removal of organic surface contaminants [133] and the environmental friendliness of the UV/Ozone technique [134–136], it is expected that this surface treatment of polymers will stay behind its

"alternatives". Most probably due to its rather low process speed as well as the higher commercial profits that can be made in the sales of other surface cleaning and activation techniques. An increase of the application of Excimer sources might be the game changer though.

6.8 Summary

Test results presented here show that the exposure to the wavelengths 253.7 nm and 184.9 nm, as generated by an ozone generating low-pressure mercury UV-light source, is generally very effective as a surface treatment for improving the adhesion, and as a result adhesive bond strength and durability of polymer (and metal) surfaces. However, changes in the sample distance to the UV-C source, wavelength used, or the ozone gas concentration as process parameters influence strongly the efficiency of the surface cleaning and activation for improved adhesive bonding.

The UV/Ozone process is, in general, very well suited for increasing the density of polar groups (and oxygen) on a polymer surface, showing an increased wetting and an increase in the adhesive bond strength as a function of treatment time. Though a too long treatment time might lead to the generation of low molecular weight oxidized molecules (LMOWMs), which may reduce the bond strength.

More than 30 years of experimental work has shown that UV/Ozone treatment by low pressure mercury light sources is very effective for increasing the initial as well as the long-term adhesive bond strength where other physical surface treatments such as corona and atmospheric plasma hardly showed any improvement. In some cases, especially when used in combination with metals, it succeeds to give increased bond strength [131] by reproducible removal of thin layers of hydrophobic contaminating materials, such as many types of greases, including finger grease, Teflon® and silicone oils, which is a characteristic that was hardly found with the other investigated physical surface treatments such as atmospheric plasma and corona.

Acknowledgements

The authors are very grateful to the following individuals for their contributions: A. Kooijman, B. Boshuizen, C. Del Grosso, S. Teixeira de Freitas, W. Wandong, D. Zarouchas, I. Vieira, F. Badan and H. Nevel. Staff members: B. Out, J. Vervloed, P. de Regt, J. Hofstede, C. de Ruijter, R. Steenbreker,

F. de Wit, R. J. Lemmen, D. Borger, M. van der Leeden, I. Cringus-Fundeanu and P. Beentjes. Management assistants: M. Oosterloo, W. Veldhoven, P. Peers and G. van der Windt. Board members: G. Frens, B. Vogelesang, A. Vlot and R. Benedictus. Faculty colleagues: R. Alderliesten, F. Oostrum, B. Grashof, D. Mainali, and all laboratory staff and workshop technicians.

References

1. M. Strobel, C. S. Lyons and K. L. Mittal (Eds.), *Plasma Surface Modification of Polymers: Relevance to Adhesion*, CRC Press, Boca Raton, FL (1994).
2. K.L. Mittal and T. Bahners (Eds.), *Laser Surface Modification and Adhesion*, Wiley–Scrivener, Beverly, MA (2015).
3. G.A. Takacs, M.J. Miri and T Kovach, Vacuum UV surface photo-oxidation of polymeric and other materials for improving adhesion: A critical review, *Rev. Adhesion Adhesives*, 8, 555-581 (2020).
4. C.A. Del Grosso, J.A. Poulis and E.R. de la Rie, The photo-stability of acrylic tri-block copolymer blends for the consolidation of cultural heritage, *Polym. Degradation Stability*, 159, 31-42 (2019).
5. G.A. El-Hiti, D.S. Ahmed, E. Yousif, O. S.A. Al-Khazrajy, M. Abdallh and S.A. Alanazi, Modification of polymers through the addition of ultraviolet absorbers to reduce aging effect of accelerated and natural irradiation, *Polymers*, 14, 20 (2022).
6. M. D. Landete-Ruiz and J. M. Martin-Martinez, Surface modification of EVA copolymer by UV treatment, *Int. J. Adhesion Adhesives*. 25, 139-145 (2005).
7. M.D. Romero-Sánchez, M.M Pastor-Blas, J. M. Martín-Matínez and M.J. Walzak, UV treatment of synthetic styrene-butadiene-styrene rubber, *J. Adhesion Sci. Technol.*,17, 25-45 (2003).
8. J.R. Vig, UV/Ozone cleaning of surfaces, in: *Treatise on Clean Surface Technology*, K.L. Mittal (Ed), pp. 1-26, Springer, Boston MA (1987).
9. J.A. Poulis, J.C. Cool and E.H.P. Logtenberg, UV/Ozone cleaning, a convenient alternative for high quality bonding preparation, *Int. J. Adhesion Adhesives*. 13, 89-96 (1993).
10. A.R. Rodríguez, L.A. Boshuizen, B.C. Rans and J.A. Poulis, The influence of grit blasting and UV/Ozone treatments on Ti-Ti adhesive bonds and their durability after sol-gel and primer application, *Int. J. Adhesion Adhesives*, 104, 1-10 (2021).
11. A.R. Rodríguez, L.A. Boshuizen, B.C. Rans and J.A. Poulis, Effect of surface morphology on the Ti-Ti adhesive bond performance of Ti6Al4V parts fabricated by selective laser melting, *Int. J. Adhesion Adhesives*, 110, 1-10 (2021).
12. N. Pichler, W. Wang, J.A. Poulis and E. Ghafoori, Surface preparations and durability of iron-based shape memory alloy adhesively-bonded joints, *Int. J. Adhesion Adhesives* (2023). Accepted, but not yet published

13. K. Jousten, *Handbook of Vacuum Technology*, pp. 463-474, John Wiley & Sons (2008).
14. J.A. Poulis, Small cylindrical adhesive bonds, PhD thesis, Delft University of Technology, Delft, The Netherlands (1993).
15. N. S. McIntyre and M.J. Walzak, New UV/ozone treatment improves adhesiveness of polymer surfaces, *Modern Plastics Int.* 25, 69-75 (1995).
16. J.R. Vig and J. LeBus, UV/Ozone cleaning of surfaces, *IEEE Trans. Parts Hybrids Packaging*, 12, 365-370 (1976).
17. Ann., Bright-Euram3, FP4, European Craft project, No. *BE-ST-2032,*UV/Ozone surface treatment of polymers for high quality adhesion in the footwear and coating industry, Grant agreement ID: BRST965055 (1996-1998).
18. L. Zafonte and R. Chiu, UV/ozone cleaning for organics removal on silicon wafers, *Proc. SPIE*, 470, 164-177 (1984).
19. M. Tabe, UV ozone cleaning of silicon substrates in silicon molecular beam epitaxy, *Appl. Phys. Lett.* 45, 1073-1075 (1984).
20. G.A. Diaz-Quijada, R. Peytavi, A. Nantel, E. Roy, M.G. Bergeron, M.M. Dumoulin and T. Veres, Surface modification of thermoplastics - towards the plastic biochip for high throughput screening devices, *Lab Chip* 7, 856-862 (2007).
21. R.H. Bradley, I.L. Clackson and D.E. Sykcs, UV/Ozone modification of wool fibre surfaces, *Appl. Surf. Sci.* 72, 143-147 (1993).
22. K. Sato, A. Ijuin, Y Imai and Y Hotta, A feasibility study on direct measurements of interaction forces between carbon fiber surfaces and other substances, *Polym. Composites*, 41, 5209-5215 (2020).
23. M.A. Downey and L.T. Drzal, Toughening of carbon fiber-reinforced epoxy polymer composites utilizing fiber surface treatment and sizing, *Composites Part A*, 90, 687-698 (2016).
24. A. Debot, V. B. Chu, D. Adeleye, J. Guillot, D. Arl, M. Melchiorre and P.J. Dale, Inkjet-printed indium sulfide buffer layer for $Cu(In,Ga)(S,Se)_2$ thin film solar cells, *Thin Solid Films* 745, 139096-139101 (2022).
25. R.A. Crandall, The use of ultraviolet light in the treatment of water in public spas and hot tubs, *J. Environmental Health*, 49, 16-23 (1986).
26. J. Wang, J. Shen, D. Ye, X. Yan, Y. Zhang, W. Yang, X. Li, J. Wang, L. Zhang and L. Pan, Disinfection technology of hospital wastes and wastewater: Suggestions for disinfection strategy during corona virus disease 2019 (COVID-19) pandemic in China, *Environmental Pollution*, 262 114665-114674 (2020).
27. M. Raeiszadeh and B. Adeli, A critical review on ultraviolet disinfection systems against COVID-19 outbreak: applicability, validation, and safety considerations, *ACS Photonics* 7, 2941-2951 (2020).
28. H. Claus, Ozone generation by ultraviolet lamps, *Photochem Photobiol* 97, 471-476 (2021).
29. Ann., Desinfektion mit UV-Strahlung, Bestell Nr. 1817, Stand 5/59, Philips Licht, Philips GmbH, Hamburg, Germany.

30. G. Knight, Monitoring of ultraviolet light sources for water disinfection, Conference Record of the 2004 IEEE Industry Applications Conference, 39th IAS Annual Meeting, Vol.2, 1016-1018 (2004).
31. C.C.E. Meulemans, The basic principles of UV–disinfection of water, *Ozone: Sci. Eng*. 9, 299-313 (1987).
32. M. van der Meer, F. van Lierop and D. Sokolov, The analysis of modern low pressure amalgam lamp characteristics, https://www.semanticscholar.org/paper/The-analysis-of-modern-low-pressure-amalgam-lamp-Meer-Lierop/8484103e410249bb329c44e6868aa71f6ab48f1a (2015).
33. C. Tuchinda, S. Srivannaboon and H.W. Lim, Photoprotection by window glass, automobile glass, and sunglasses, *J. Am. Acad. Dermatol.*, 54, 845-854 (2006).
34. UV-Technik Special Lampen GmbH, Wümbach, Germany (2015).
35. U. Kogelschatz, Dielectric-barrier discharges: Their history, discharge physics, and industrial applications, *Plasma Chem. Plasma Proc.*, 23, 1-46 (2003).
36. A. Fujioka, K. Asada, H. Yamada, T. Ohtsuka, T. Ogawa, T. Kosugi, D. Kishikawa and T. Mukai, High-output-power 255/280/310 nm deep ultraviolet light-emitting diodes and their lifetime characteristics *Semicond. Sci. Technol.*, 24, 084005- 084010 (2014).
37. F. Anwar, F.N. Chaudhry, S. Nazeer, N. Zaman and S. Azam, Causes of ozone layer depletion and its effects on human: Review, *Atmospheric Climate Sci.* 6, 129-134 (2016).
38. J.D. McClurkin and D.E. Maier, Half-life of ozone as a function of air conditions and movement, Proceedings 10th Int. Working Conf. on Stored Product Protection, 425 (2010).
39. R. G. Rice and N. Aharon, Introduction, in: *Handbook of Ozone Technology and Applications*, Vol. 1, pp. 1-9, R. G. Rice and N. Aharon (Eds), Ann Arbor Science Publishers, Ann Arbor, MI (1982).
40. Ann., WHO, Environmental Health Criteria 7; Photochemical Oxidants, World Health Organization, Geneva (1979).
41. C. Mühlhan and H. Nowack, Plasma pretreatment of polypropylene for improved adhesive bonding, *Surf. Coatings Technol.*, 1-3, 1107-1111 (1998).
42. A. Popelka, I. Novak and I. Krupa, Polyolefin adhesion modifications, in: *Polyolefin Compounds and Materials, Fundamentals and Industrial Applications,* M. Al-Ali AlMa´adeed and I. Krupa, (Eds), pp. 201-230, Springer Series on Polymer and Composite Materials, Heidelberg (2016).
43. L.F. MacManus, M.J. Walzak and N.S. McIntyre, Study of ultraviolet light and ozone surface modification of polypropylene, *J. Polym. Sci, Part A: Polym. Chem.*, 37, 2489-2501 (2000).
44. R. Ono, Y. Nakagawa, Y. Tokumitsu, H. Matsumoto and T. Oda, Effect of humidity on the production of ozone and other radicals by low-pressure mercury lamps, *J. Photochem. Photobiol.* A 274, 13-19 (2014).
45. E. Arikan, J. Holtmannspötter, F. Zimmer, T. Hofmann and H-J Gudladt, The role of chemical surface modification for structural adhesive bonding

on polymers – washability of chemical functionalization without reducing adhesion, *Int. J. Adhesion Adhesives*, 95, 1-12 (2019).
46. S. Sapieha, J. Cerny, J. E. Klemberg-Sapieha and L. Martinu, Corona versus low pressure plasma treatment: Effect on surface properties and adhesion of polymers, *J. Adhesion*, 42, 91-102 (1993).
47. M.J. Walzak, S. Flynn, R. Foerch, J.M. Hill, E. Karbashewski, A. Lin and M. Strobel, UV and ozone treatment of polypropylene and poly(ethylene terephthalate), *J. Adhesion Sci. Technol.* 9, 1229-1248 (1995).
48. M.M. Makogon, Yu. N. Ponomarev and B.A. Tikhomirov, The problem of water vapour absorption in the UV spectral range, *Atmospheric Oceanic Optics*, 26, 45-49 (2013).
49. J.M. Hill, E. Karbashewski, A. Lin, M. Strobel and M.J. Walzak, Effects of aging and washing on UV and ozone-treated poly(ethylene terephthalate) and polypropylene, *J. Adhesion Sci. Technol.* 9, 1575-1591 (1995).
50. W. Wang, S.T. de Freitas, J.A. Poulis and D. Zarouchas, A review of experimental and theoretical fracture characterization of bi-material bonded joints, *Composites Part B*: 206, 108537-108551 (2021).
51. S. Bok, G-H. Lim and B. Lim, UV/ozone treatment for adhesion improvement of copper/epoxy interface, *J. Ind. Eng. Chem.* 46, 199-202 (2017).
52. K.L. Mittal, The role of the interface in adhesion phenomena, *Polym. Eng. Sci.* 17, 467-473 (1977)
53. E.M. Petrie, *Handbook of Adhesives and Sealants,* 2nd edition, pp. 267-270, McGraw Hill, New York (2007).
54. L.W. McKeen, Introduction to the weathering of plastics, in: *The Effect of UV-Light and Weather on Plastics and Elastomers*, PDL Handbook Series, third edition, S. Ebnesajjad (Ed.), pp.17-41, William Andrew Publishing, Norwich (2013).
55. G.A. El-Hiti, D.S. Ahmed, E. Yousif, O.S.A. Al-Khazrajy, M. Abdallh and S.A. Alanazi, Modifications of polymers through the addition of ultraviolet absorbers to reduce the aging effect of accelerated and natural irradiation, *Polymers*, 14, 20 (2022).
56. T. Ojeda, A. Freitas, K. Birck, E. Dalmolin, R. Jacques, F. Bento and F. Camargo, Degradability of linear polyolefins under natural weathering. *Polym. Degrad. Stab.*, 96, 703–707 (2011).
57. J.G. Neevel, The identification of van Gogh's inks for drawing and writing, in: *Accelerated Aging: Photochemical and Thermal Aspects*, *Research in Conservation*, R.L. Feller (Ed.), pp. 23, 129-141, J. P. Getty Trust (1994).
58. M. Strobel, M.J. Walzak, J.M. Hill, A. Lin, E. Karbashewski and C.S. Lyons, A comparison of gas-phase methods of modifying polymer surfaces, *J. Adhesion Sci. Technol.* 9, 365-383 (1995).
59. H.S. Choi, V.V. Rybkin, V.A. Titov, T.G. Shikova and T.A. Ageeva, Comparative actions of a low pressure oxygen plasma and an atmospheric pressure glow discharge on the surface modification of polypropylene, *Surf. Coatings Technol.* 200, 4479-4488 (2006).

60. B.K. Kim, K.S. Kim, C.E. Park and C.M. Ryu, Improvement of wettability and reduction of aging effect by plasma treatment of low-density polyethylene with argon and oxygen, *J. Adhesion Sci. Technol.* 16, 509-521 (2002).
61. D. Briggs and M.P. Seah, (Eds.), *Practical Surface Analysis – Vol. 1: Auger and X-ray Photoelectron Spectroscopy*, 2nd ed., John Wiley & Sons (1990).
62. Ann., Operators Multipak Software Manual – version 6.0, Physical Electronics Inc. (1998).
63. American Society for Testing and Materials standard practice for checking the operating characteristics of X-ray photoelectron spectrometers (E902-82), *Surf. Interf. Anal.*, 10, 55-57 (1987).
64. D.A. Shirley, High-resolution X-Ray photoemission spectrum of the valence bands of gold, *Phys. Rev. B*, 5, 4709-4714 (1972).
65. NIST Standard Reference Database 20, Version 3.5 (Web Version, 2007), http://srdata.nist.gov/xps/
66. S. Oswald, X-ray photoelectron spectroscopy in analysis of surfaces, in: *Encyclopedia of Analytical Chemistry*, R.A. Meyers (Ed.), pp. 1-49, John Wiley & Sons Ltd, online library (2013).
67 J. Oelichmann, Surface and depth-profile analysis using FTIR spectroscopy, *Zeitschrift Analytische Chemie*, 333, 353-359 (1989).
68. W. Wang, J.A. Poulis, S. Teixeira De Freitas and D. Zarouchas, Surface pretreaments on CFRP and titanium for manufacturing adhesively bonded bi-material joints, Proc. 18th European Conf. on Composite Materials, Athens,1-8 (2018).
69. A. Einstein, On a heuristic point of view about the creation and conversion of light, *Annalen der Physik*, 17, 132-148 (1905).
70. M. Romand, F.Gaillard, M. Charbonnier, N.S. Prakash, L. Deshayes and I. Linossier, Adhesion science and surface analysis: Typical examples, *J. Adhesion*, 55, 1-16 (1995).
71. R. Ledesma, W. Yost, F. Palmieri, D. Cataldo and J. Connel, Correlation of optically stimulated electron emission with failure mode of adhesively bonded epoxy composites, *Int. J. Adhesion Adhesives* 84, 257-264 (2018).
72. G.D. Davis, Contamination of surfaces: Origin, detection and effect on adhesion, *Surf. Interf. Anal.* 20, 368 – 372 (1993).
73. J. Wang, Y. Wu, Y. Cao, G. Li and Y. Liao, Influence of surface roughness on contact angle hysteresis and spreading work, *Colloid Polym. Sci.* 298, 1107-1112 (2020).
74. F.M. Etzler, Determination of the surface free energy of solids: A critical review, *Rev. Adhesion Adhesives*, 1, 3-45 (2013).
75. F.M. Etzler, Characterization of surface free energies and surface chemistry of solids, in: *Contact Angle, Wettability and Adhesion*, Vol. 3, K.L. Mittal (Ed.) pp. 219-264, CRC Press, Boca Raton, FL (2003).
76. D.K. Owens and R.C. Wendt, Estimation of the surface free energy of polymers, *J. Appl. Polym. Sci.* 13, 1741-1747 (1969).

77. C.W. Karl, A.E. Krauklis, A. Lang and U. Giese, Characterization of rough PTFE surfaces by the modified Wilhelmy balance technique, *Polymers* 12, 1528 (2020).
78. D.A. Bolon and C.O. Kunz, Ultraviolet depolymerisation of photoresist polymers, *Polym. Eng. Sci.* 12, 109-111 (1972).
79. M.C. van der Leeden and G. Frens, Surface properties of plastic materials in relation to their adhering performance, *Advanced Eng. Mater.* 4, 280-289 (2002).
80. M.L. Sham, J. Li, P. Ma and J.K. Kim, Cleaning and functionalization of polymer surfaces and nanoscale carbon fillers by UV/Ozone treatment: a review, *J. Composite Mater.* 43, 1537-1564 (2009).
81. C-W. Tsao and D.L. De Voe, Bonding of thermoplastic polymer microfluidics, *Microfluidics Nanofluidics* 6, 1-16 (2009).
82. Y. Jia, H. Asahra, Y. Hsu, T-A. Asoh and H. Uyama, Surface modification of polycarbonate using the light-activated chlorine dioxide radical, *Appl. Surf. Sci.* 530, 147202 (2020).
83. Y. Hong, Z. He, N.S. Lennhoff, D.A. Banach and J. Kanicki, Transparent flexible plastic substrates for organic light –emitting devices, *J. Electronic Mater.* 33, 312-320 (2004).
84. A.J. Yáñez-Pacios and J.M. Martín-Martínez, Surface modification and adhesion of wood-plastic composite (WPC) treated with UV/ozone, *Composite Interfaces*. 25, 127-149 (2018).
85. K.S.G. Krishman, O. Obertram and O. Seibel, Review of hybrid laminar flow control systems, *Progr. Aerospace Sci.* 93, 24-52 (2017).
86. Ann., European Clean Sky project "Titanium Composite Adhesive Joints (TICOAJO)", Clean Sky 2 Joint Undertaking under the European Union's Horizon 2020 research and innovation program under grant agreement No 7377856.
87. P. Molitor, V. Barron and T. Young, Surface treatment of Titanium for adhesive bonding to polymer composites: a review, *Int. J. Adhesion Adhesives* 21, 129-136 (2001).
88. B Kolesnikov, L. Herbeck and A. Fink, CFRP/titanium hybrid material for improving composite bolted joints, *Composite Structures* 83, 368-380 (2008).
89. S.T. de Freitas and J. Sinke, Test method to assess interface adhesion in composite bonding, *Appl. Adhesion Sci* 3, 1-13 (2015).
90. Standard test method for floating roller peel resistance of adhesives, ASTM D 3167-10 (2017).
91. S. Teixeira de Freitas, D. Zarouchas and J.A. Poulis, The use of acoustic emission and composite peel tests to detect weak adhesion in composite structures, *J. Adhesion* 94, 743-766 (2018).
92. E.M. Petrie, *Handbook of Adhesives and Sealants*, 2nd edition, pp. 232-234, McGraw Hill, New York (2007).
93. A.J. Kinloch, *Adhesion and Adhesives: Science and Technology*, pp. 103-105, Chapman and Hall, New York (1990).

94. G.D. Davis, Surface treatments of selected materials, in: *Handbook of Adhesion Technology*, Vol. 1, L.F.M. da Silva, A. Öchsner and R.D. Adams (Eds), pp.171-173, Springer-Verlag, Berlin, Heidelberg (2011).
95. M. Saeedifar, M.N. Saleh, P. Nijhuis, S.T. de Freitas and D. Zarouchas, Damage assessment of a titanium skin adhesively bonded to carbon fiber-reinforced plastic omega stringers using acoustic emission, *J. Structural Health Monitoring* 2, 407-423 (2021).
96. N.Z. Tomić, M.N. Saleh, S.T. de Freitas, A. Živković, M. Vuksanović, J.A. Poulis and A. Marinković, Enhanced interface adhesion by novel eco-epoxy adhesives based on the modified tannic acid on Al and CFRP adherends, *Polymers* 12, 1541 (2020).
97. G. Bockmair and K. Kranzeder, Surface protection for aircraft maintenance by means of zinc-rich primers. *Advanced Mater. Res.* 138, 41–46 (2010).
98. L.P. Haack, A.M. Straccia. J.W Holubka, A. Bhurke, M. Xie and L. T. Drzal. Chemistry of surface modification with UV/Ozone for improved intercoat adhesion in multi-layered coating systems, *Surf. Interf. Anal.* 29, 829-836 (2000).
99. Paints and varnishes - cross-cut test, ISO 2409 (1992).
100. Standard test method for apparent shear strength of single-lap-joint adhesively bonded metal specimens by tension loading (metal-to-metal), ASTM D-1002-10 (2019).
101. Adhesives - Determination of tensile strength of butt joints, EN 15870 (2009).
102. H. Neevel, Logwood writing inks: History, production, forensics, and use, *Restaurator. Int. J. Preservation of Library and Archival Mater.*, 42, 169-191 (2021).
103. J.G. Neevel, The identification of van Gogh's inks for drawing and writing, in: *The Identification of van Gogh's Inks*, M. Vellekoop, M. Geldof, E. Hendriks, L. Jansen and A. de Tagle (Eds), pp. 420-436, Yale University Press, New Haven and London (2013).
104. K. Efimenko, W.E. Wallace and J. Genzer, Surface modification of Sylgard-184 Poly(dimethyl siloxane) networks by ultraviolet and ultraviolet/Ozone treatment, *J. Colloid Interface Sci.*, 254, 306-315 (2002).
105. K-S Koh, J. Chin, J. Chia and C-L Chiang, Quantitative studies on PDMS-PDMS interface bonding with piranha solution and it swelling effect, *Micromachines*, 3, 427-441 (2012).
106. Y Berdichevsky, J. Khandurina, A. Guttman and Y.-H Lo, UV/ozone modification of poly(dimethylsiloxane) microfluidic channels, *Sensors Actuators B* 97, 402-408 (2004).
107. H. Hillborg and U.W. Gedde, Hydrophobicity changes in silicone rubbers, *IEEE Trans. Dielectrics Electrical Insulation*, 6, 703-717 (1999).
108. M.J. Owen and P.J. Smith, Plasma treatment of polydimethylsiloxane, *J. Adhesion Sci Technol.* 8, 1063-1075 (1994).

109. J. Friedrich, *Metal-Polymer Systems: Interface Design and Chemical Bonding*, pp. 173-237, Wiley-VCH Verlag (2018).
110. R. Oostrom, T.J. Ahmed, J.A. Poulis and H.E.N. Bersee, Adhesion performance of UHMWPE after different surface modification techniques, *Medical. Eng. Phys.* 28, 323-330 (2006).
111. L. Mathieson and R.H. Bradley, Improved adhesion to polymers by UV/ozone surface oxidation, *Int. J. Adhesion Adhesives*, 16, 29-31 (1996).
112. A.M. Guedes Pinto, A.G. Magalhães, F.G. da Silva and A.P. Monterio Baptista, Shear strength of adhesively bonded polyolefins with minimal surface preparation, *Int. J. Adhesion Adhesives*. 28, 452-456 (2008).
113. H. Tsubaki, S. Inokuchi and T. Ogawa, Joined body and method of producing joined body, US Patent 8974902B2, assigned to Nitto Denko Corporation, Osaka, Japan (2015).
114. E. Orgilés-Calpena, F. Arán-Aís, A M. Torró-Palau and M.A. Martínez Sánchez, Adhesives in the footwear industry: A critical review, *Rev. Adhesion Adhesives*, 7, 69-91 (2019).
115. K.A. Williams, L.T. Germinario and R. Eagan, Adhesion and gasoline resistance performance properties of chlorinated and non-chlorinated polyolefin adhesion promoters and blends for TPO substrates, Proc. Int. Coatings for Plastics Symposium, Troy, MI, pp. 1-15 (2003).
116. PFQD, quick drying residue –free solvent, PT Technologies, Ireland.
117. E.M. Petrie, *Handbook of Adhesives and Sealants,* 2nd edition, pp. 890-892, McGraw Hill, New York (2007).
118. C.Q. Sun, D. Zhang and L.C. Wadsworth, Corona treatment of polyolefin films-A review, *Adv. Polym. Technol.*, 18, 171-180 (1999).
119. M. Kłonica, J. Kuczmaszewski, M. Kwiatkowski and J. Ozonek, Polyamide 6 surface treatment layer following ozone treatment, *Int. J. Adhesion Adhesives*, 64, 179-187 (2016).
120. E.M. Liston, L. Martinu and R. Wertheimer, Plasma surface modification of polymers for improved adhesion, *J. Adhesion Sci. Technol.*, 7, 1091-1127 (1993).
121. P. Blais, D.J Carlsson and D.M. Wiles, Effects of corona treatment on composite formation. Adhesion between incompatible polymers, *J. Appl. Polym. Sci*. 15, 129-143 (1971).
122. N. Anagreh, L. Dorn and C. Bilke-Krause, Low-pressure plasma pretreatment of polyphenylene sulphide (PPS) surfaces for adhesive bonding, *Int. J. Adhesion. Adhesives*, 28, 16-22 (2008).
123. M. Frascio, C. Mandolfino, F. Moroni, M. Jilich, A. Lagazzo, M. Pizzorni, L. Bergonzi, C. Morano, M. Alfano and M. Avalle, Appraisal of surface preparation in adhesive bonding of additive manufactured substrates, *Int. J. Adhesion Adhesives*. 106, 102802 (2021).
124. Standard test method for peel resistance of adhesives, (T-Peel test), ASTM D 1876-08 (2016).

125. R. Kapica, J. Tyckowski, J. Balcerzak, M. Makowski, J. Sielski and E. Worwa, Enhancing adhesive joints between commercial rubber (SBS) and polyurethane by low-pressure plasma surface modification, *Int. J. Adhesion Adhesives* 95, 102415 (2019).
126. C.W. Karl, W. Rahimi, S. Kubowicz, A. Lang, H. Geisler and U. Giese, Surface modification of ethylene propylene diene terpolymer rubber by plasma polymerization using organosilicon precursors, *ACS Appl. Polym. Mater* 2, 3789-3796 (2020).
127. M.D. Romero-Sánchez and J.M. Martín-Martínez, UV-Ozone surface treatment of SBS rubbers containing fillers: Influence of the filler nature on the extent of surface modification and adhesion, *J. Adhesion Sci. Technol.* 22, 147-168 (2008).
128. J.H. Moraes, A.S. da Silva Sobrinho, H.S. Maciel, J.C.N Dutra, M. Massi, S.A.C. Mello and W.H. Schreiner, Surface improvement of EPDM rubber by plasma treatment, *J. Phys. D: Appl. Phys*. 40, 7747-7752 (2007).
129. K.F. Grythe and F.K. Hansen, Surface modification of EPDM rubber by plasma treatment, *Langmuir* 22, 6109-6124 (2006).
130. M. Hamdi and J.A. Poulis, Effect of UV/Ozone treatment on the wettability and adhesion of polymeric systems, *J. Adhesion*, 97, 651-671 (2021).
131. E.M. Petrie, *Handbook of Adhesives and Sealants,* 2nd edition, pp. 62-64, McGraw Hill, New York (2007).
132. A.C. Marques, A. Mocanu, N.Z. Tomić, S. Balos, E. Stammen, E. Lundevall, S.T. Abrahami, R. Günther, J.M.M. de Kok and S. Teixera de Freitas, Review on adhesives and surface treatments for structural applications, *Materials* 13, 1-43 (2020).
133. M.A Moyano and J.M Martín-Martínez, Surface treatment with UV/ozone to improve adhesion of vulcanized rubber formulated with an excess of processing oil, *Int. J. Adhesion Adhesives*. 55, 106 –113 (2014).
134. M. de Boo, Solvents replaced by UV irradiation and ozone, *Outlook*, 2, 17-20 (1993).
135. J. Seo, W.S. Chang and T-S Kim, Adhesion improvement of graphene/copper interface using UV/ozone treatments, *Thin Solid Films* 584, 170-175 (2015).
136. R. Kohli, Applications of UV/Ozone cleaning technique for removal of surface contaminants, in: *Developments in Surface Contamination and Cleaning*, Vol. 11, R. Kohli and K.L. Mittal (Eds.), Chapter 9, Elsevier, Oxford, UK (2019).